Distinct medial amygdala oxytocin receptor neurons projections respectively control consolation or aggression in male mandarin voles

Supplementary Figures

Supplementary Fig. 1

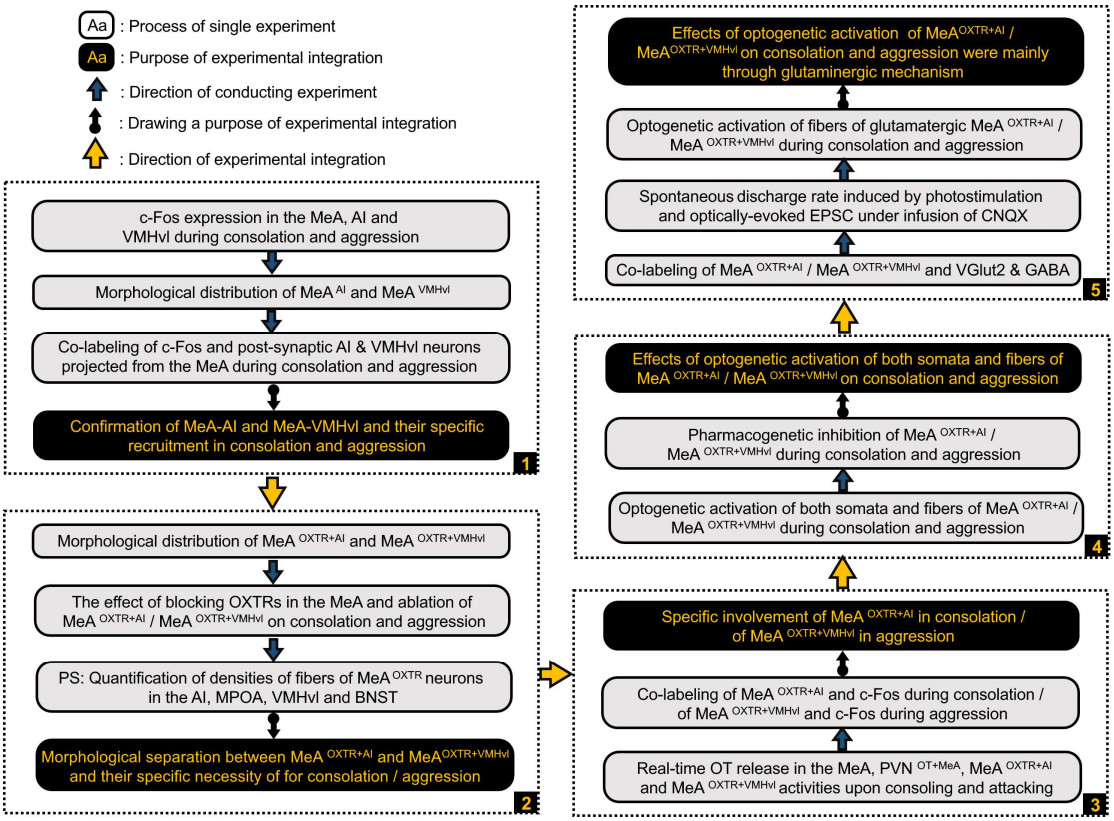

Supplementary Fig. 1 | The flow chart of experimental run and corresponding purpose in the present study.

Arabic numerals from 1 to 5 represent the five major experiments in this study. AI = anterior insula; MPOA = Medial preoptic area; VMHvl = ventrolateral aspect of ventromedial hypothalamus; BNST = bed nucleus of the stria terminalis; VGlut2 = vesicular glutamate transporters 2; CNQX = 6-cyano-7-nitroquinoxaline-2,3-dione, AMPA receptor antagonist.

Supplementary Fig. 2

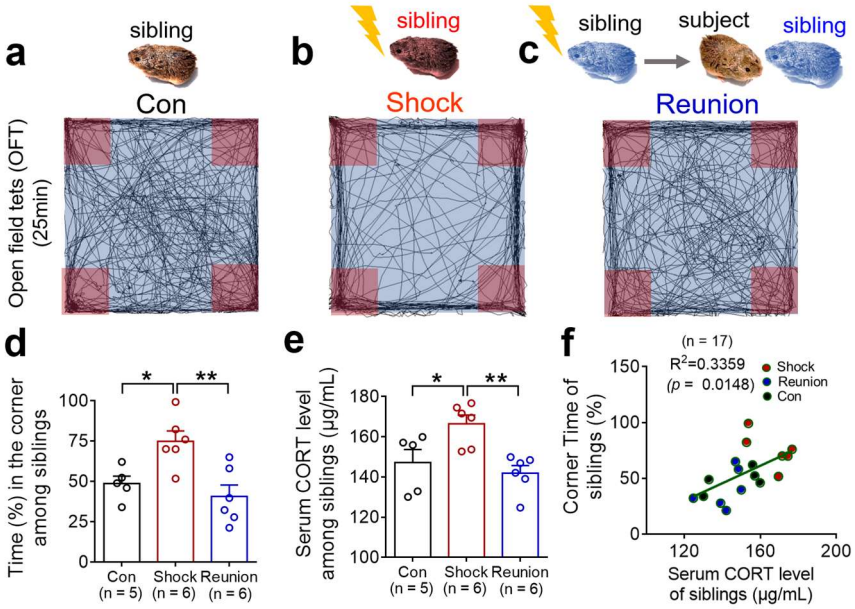

Supplementary Fig. 2 | Examination of stress buffering effect of consolation among male sibling voles by 25-min open field test (OFT).

a–**c** Sibling voles were either group-housed (Con, n = 5 voles, **a**), remained alone (Shock, n = 6 voles, **b**) or allowed to social interaction with subjects and receive consolation (Reunion, n = 6 voles, **c**) after electric foot-shocks (10 repetitions, 3s, 0.8 mA, 2-min interval). The corresponding track diagrams showed siblings' locomotion in the corners during OFT. The corresponding track diagrams showed siblings' locomotion in the corners (dark red shadow) during OFT. **d** Time percentage of corners in the OFT among groups. Siblings were allowed to freely move on the platform for 25 min. Con versus Shock, $p = 0.036$; Shock versus Reunion, $p = 0.004$. **e** Serum CORT level among groups. Con versus Shock, $p = 0.043$; Shock versus Reunion, $p = 0.007$. **f** Correlation analysis between percentage of corner time and CORT level among all siblings (N = 17). $R^2 = 0.580$, $p = 0.0148$. $^{**}p < 0.01$, $^{*}p < 0.05$. Data analyzed by One-way ANOVA with Sidak's multiple comparison test (**d**, **e**) and Pearson Correlation Analysis (**f**). Data are presented as the means +/- SEM. Statistical details are presented in Supplementary Data. 1 file. Source data are provided as a Source Data file. CORT = cortisol.

Supplementary Fig. 3

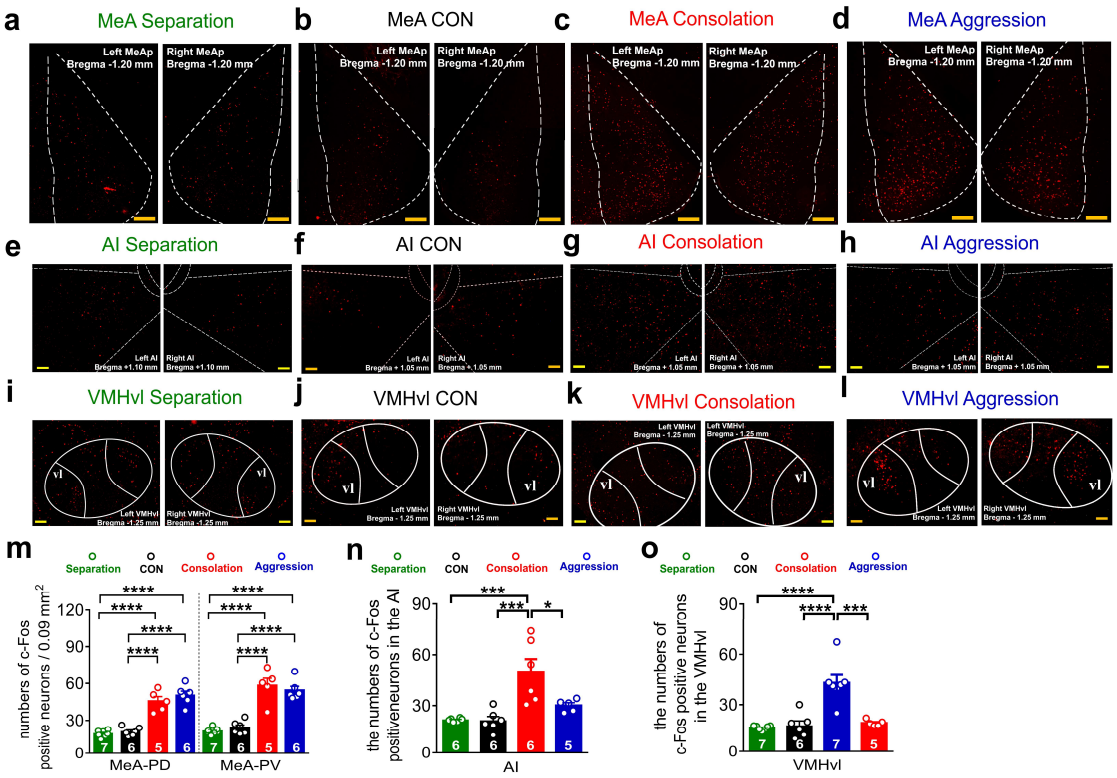

Supplementary Fig. 3 | Effect of consolation and aggression on c-Fos expression in the AI, VMHvl and MeA neurons.

a–**d** Representative images of c-Fos positive cells (Cy3, red) in the MeA after the separation treatment (Separation, n = 7 voles, **a**), control treatment (CON, n = 6 voles, **b**), consolation test (Consolation, n = 5 voles, **c**) and resident-intruder paradigm (Aggression, n = 6 voles, **d**). Scale bars, 200 μm. **e**–**h** Representative images of c-Fos positive cells in the AI in the Separation (n = 6 voles, **e**), CON (n = 6 voles, **f**), Consolation (n = 6 voles, **g**) and Aggression (n = 5 voles, **h**). Scale bars, 100 μm. **i**–**l** Representative images of c-Fos positive cells in the VMHvl in the Separation (n = 7 voles, **i**), CON (n = 6 voles, **j**), Aggression (n = 7 voles, **k**) and Consolation (n = 5 voles, **l**) groups. Scale bars, 100 μm. **m** Quantitative distinction of numbers of c-Fos positive cells in the posterior dorsal (PD) and posterior ventral (PV) subregions among groups. At the PD, Separation versus Consolation, $p < 0.0001$; Separation versus Aggression, $p < 0.0001$; CON versus Consolation, $p < 0.0001$; CON versus Aggression, $p < 0.0001$. At the PV, Separation versus Consolation, $p < 0.0001$; Separation versus Aggression, $p < 0.0001$; CON versus Consolation, $p < 0.0001$; CON versus Aggression, $p < 0.0001$. **n** Quantitative distinction of the numbers of c-Fos positive cells in the AI among groups. Separation versus Consolation, $p = 0.0007$; CON versus Consolation, $p = 0.0006$; Consolation versus Aggression, $p = 0.0266$. **o** Quantitative distinction of the numbers of c-Fos positive cells in the VMHvl among groups. Separation versus Aggression, $p < 0.0001$; CON versus Aggression, $p < 0.0001$; Consolation versus Aggression, $p = 0.0002$. $^{****}p < 0.0001$, $^{***}p < 0.001$, $^{**}p < 0.01$, $^{*}p < 0.05$. Data analyzed by One-way ANOVA with Sidak's multiple comparison test (**m**–**o**). Data are presented as the means +/- SEM. Statistical details are presented in Supplementary Data. 1 file. Source data are provided as a Source Data file.

Supplementary Fig. 4

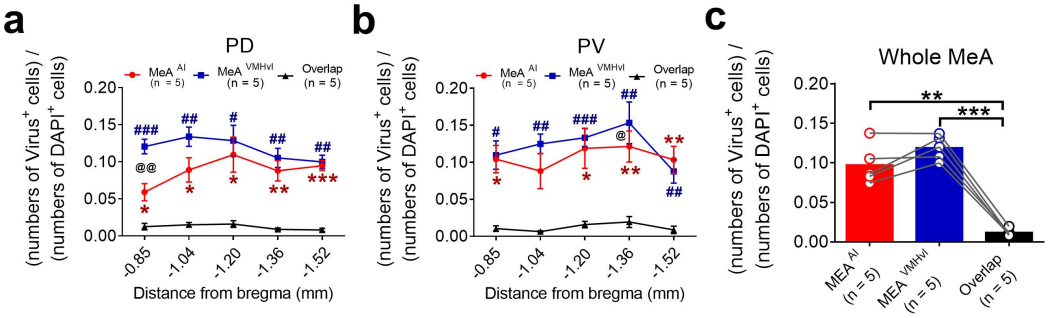

Supplementary Fig. 4 | The proportions of MeA^{AI}, MeA^{VMHvl}, MeA $^{AI+VMHvl}$ at the both PD and PV subregions along the anteroposterior axis and the proportions of MeA^{AI}, MeA^{VMHvl}, MeA $^{AI+VMHvl}$ in the whole MeA.

a Proportions of MeA^{AI}, MeA^{VMHvl}, MeA$^{AI+VMHvl}$ (Overlap) at the MeA posterior dorsal (PD) along the anteroposterior axis. At the same bregma site. *, $^{\#}$ and $^{@}$ implie significant difference between the Overlap and MeA^{AI}, between the Overlap and MeA^{VMHvl}, and between the MeA^{AI} and MeA^{VMHvl}, respectively. At bregma -0.85, $^{*}p = 0.0143$, $^{\#\#\#}p = 0.0002$, $^{@@}p = 0.0055$; At bregma -1.04, $^{*}p = 0.0186$; $^{\#\#}p = 0.0044$; At bregma -1.20, $^{*}p = 0.0276$, $^{\#}p = 0.0127$; At bregma -1.36, $^{**}p = 0.0097$, $^{\#\#}p = 0.0036$; At bregma -1.52, $^{***}p = 0.0003$, $^{\#\#}p = 0.0028$. **b** Proportions of MeA^{AI}, MeA^{VMHvl}, Overlap at the MeA posterior dorsal (PV) along the anteroposterior axis. At bregma -0.85, $^{*}p = 0.0126$, $^{\#}p = 0.0124$; At bregma -1.04, $^{*}p = 0.0327$, $^{\#\#}p = 0.0027$; At bregma -1.20, $^{*}p = 0.0327$, $^{\#\#\#}p = 0.0009$; At bregma -1.36, $^{**}p = 0.0055$, $^{\#\#}p = 0.0093$, $^{@}p = 0.0422$; At bregma -1.52, $^{**}p = 0.0094$, $^{\#\#}p = 0.0073$. **c** Proportions of MeA^{AI}, MeA^{VMHvl}, MeA $^{AI+VMHvl(Overlap)}$. MeA^{AI} versus MeA^{Overlap}, $p = 0.002$; MeA^{VMHvl} versus MeA^{Overlap}, $p < 0.0001$. $^{***}p < 0.001$, $^{**}p < 0.01$, $^{*}p < 0.05$. $^{\#\#\#}p < 0.001$, $^{\#\#}p < 0.01$, $^{\#}p < 0.05$, $^{@}p < 0.05$, $^{@@}p < 0.01$. Data analyzed by Repeated measure two-way ANOVA with Sidak's multiple comparison test (**a**, **b**) and Repeated measure one-way ANOVA with Sidak's multiple comparison test (**c**). Data are presented as the means +/- SEM. Statistical details are presented in Supplementary Data. 1 file. Source data are provided as a Source Data file.

Supplementary Fig. 5

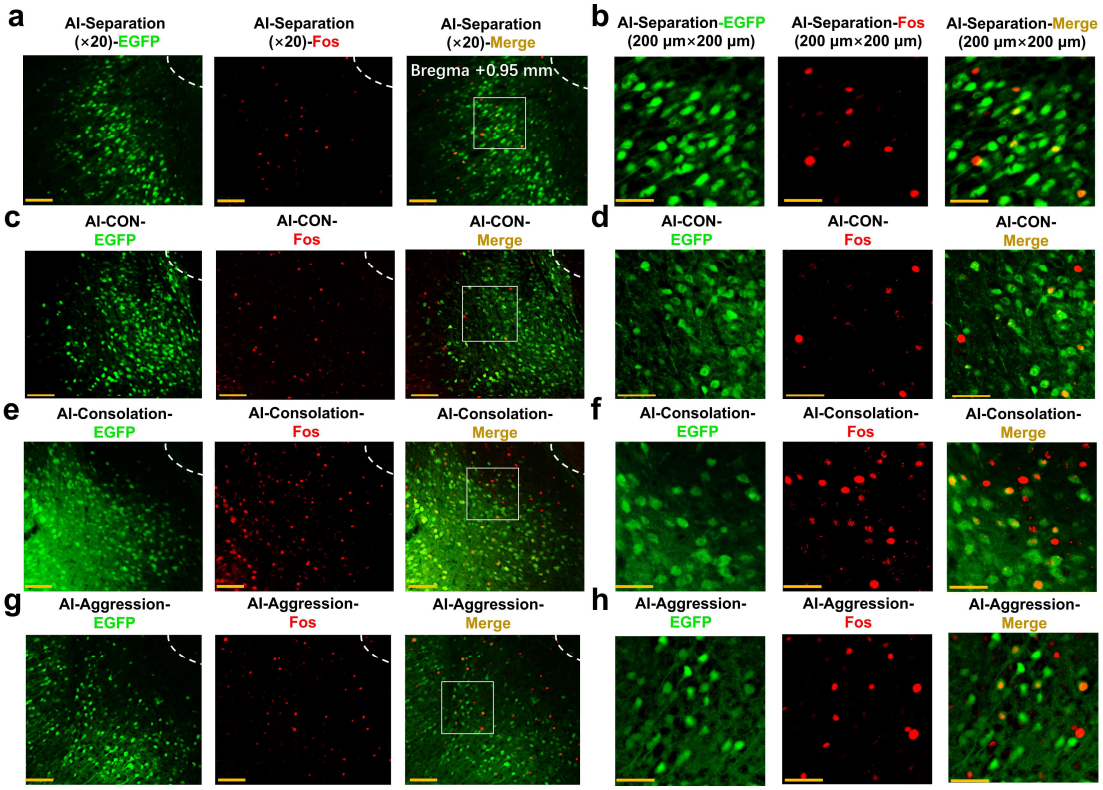

Supplementary Fig. 5 | The corresponding individual channels' images from representative overlapped images of anterograde virus and c-Fos at the AI ($AI^{MeA+Fos}$) in the Separation, CON, Consolation and Aggression groups.

The enlarged views of the selected white boxed areas (200 μm × 200 μm). Scale bars, 100 μm in (**a**), (**c**), (**e**) and (**g**), 50 μm in (**b**), (**d**), (**f**) and (**h**).

Supplementary Fig. 6

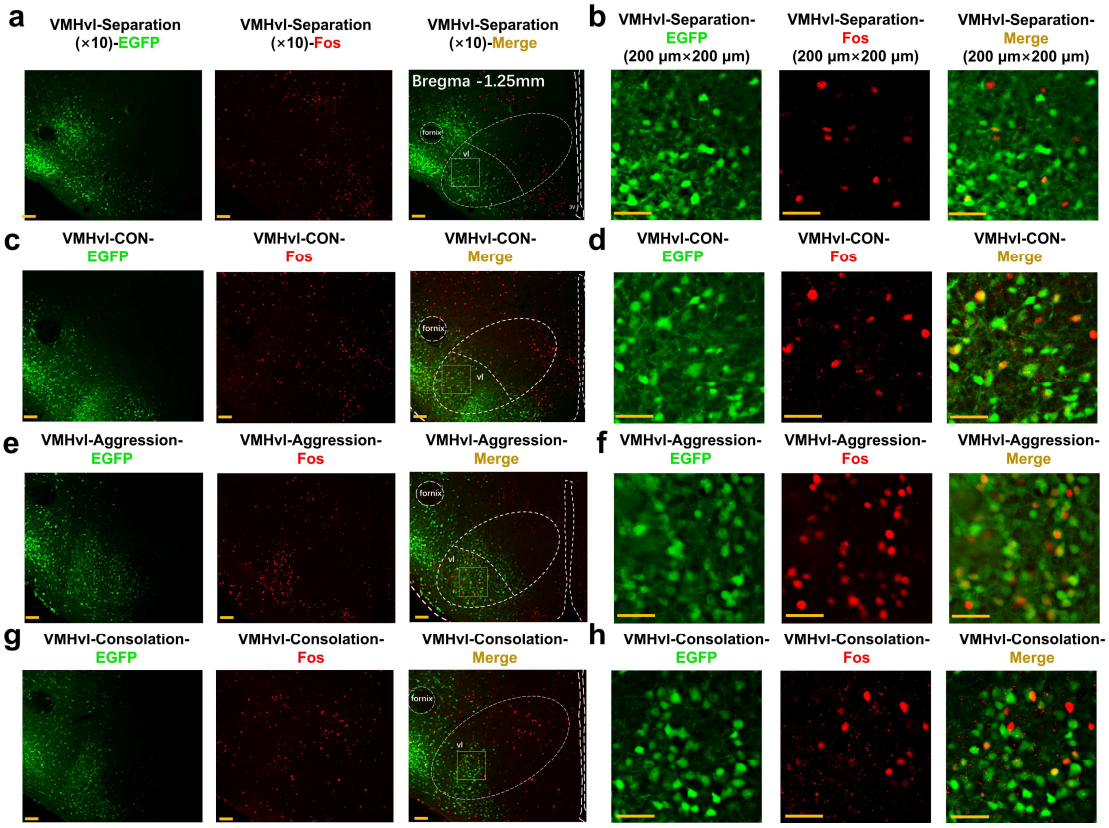

Supplementary Fig. 6 | The corresponding individual channels' images from representative overlapped images of anterograde virus and c-Fos at the VMHvl (VMHvl$^{MeA+Fos}$) in the Separation, CON, Consolation and Aggression groups.

The enlarged views of the selected white boxed areas (200 μm × 200 μm). Scale bars, 100 μm in (**a**), (**c**), (**e**) and (**g**), 50 μm in (**b**), (**d**), (**f**) and (**h**).

Supplementary Fig. 7

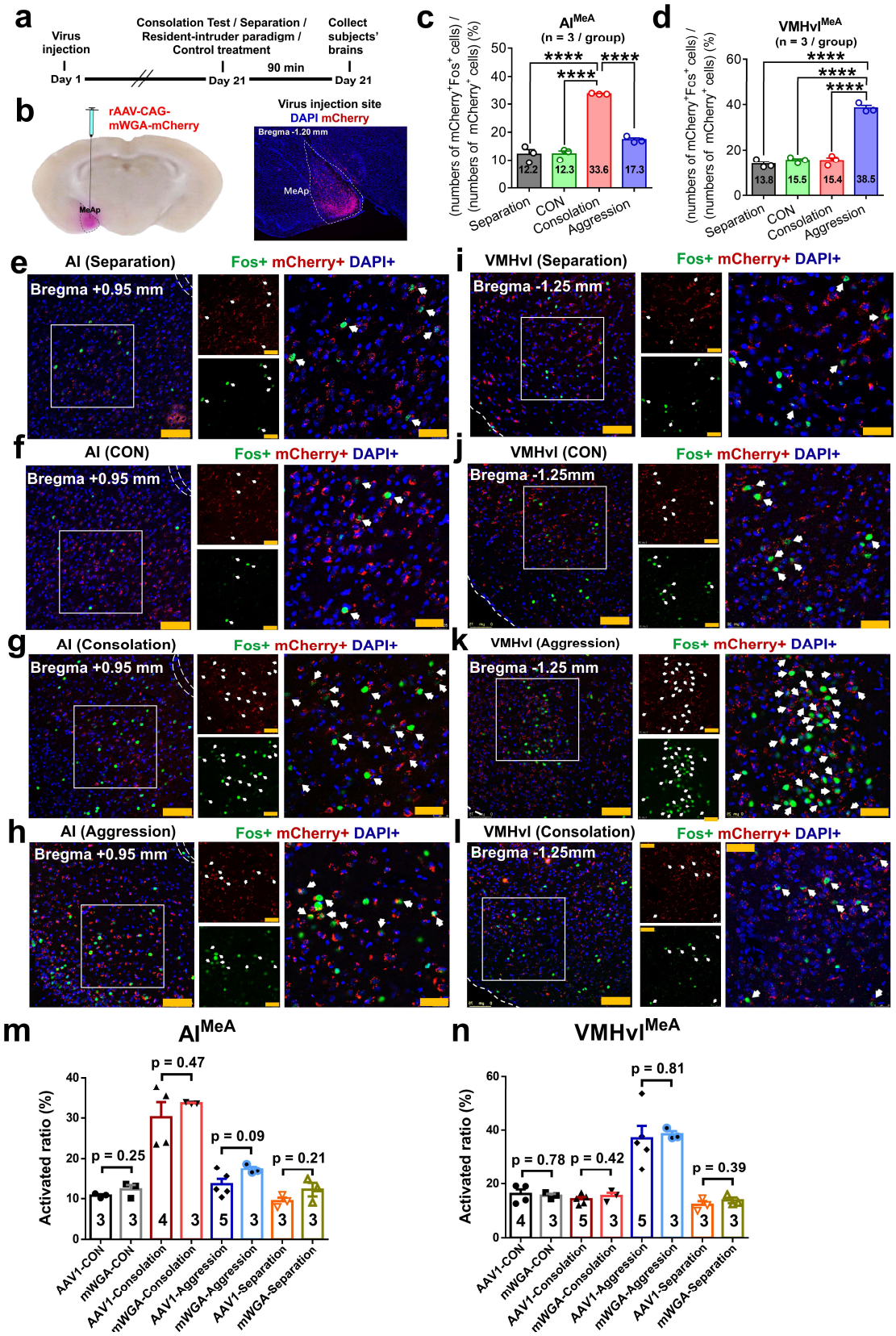

Supplementary Fig. 7 | Using fluorescent anterograde trans-synaptic tracer (mWGA-mCherry) and c-Fos labeling to map post-synaptic (AI and VMHvl) neuronal activity from the MeA during different behaviors.

a, **b** Diagram showing injection schedule (**a**) and injection site (**b**). Scale bars, 500 μm. 12 independent repetitions with similar results. **c** Comparison of percentage of mCherry and c-Fos co-labeling AI neurons in whole anterograde virus-marked neurons between the Separation, CON, Consolation and Aggression groups. Separation versus Consolation, $p < 0.0001$; CON versus Consolation, $p < 0.0001$; Consolation versus Aggression, $p < 0.0001$; Separation versus CON, $p > 0.9999$. **d** Comparison of percentage of mCherry and c-Fos co-labeling VMHvl neurons in whole anterograde virus-marked neurons among groups. Separation versus Aggression, $p < 0.0001$; CON versus Aggression, $p < 0.0001$; Consolation versus Aggression, $p < 0.0001$; Separation versus CON, $p = 0.8535$. **e**–**h** Representative overlapped images of anterograde monosynaptic virus (mCherry, red) and c-Fos (AF488, green) at the AI in Separation (**e**), CON (**f**), Consolation (**g**) and Aggression (**h**). **i**–**l** Representative overlapped images of anterograde virus and c-Fos at the VMHvl in Separation (**i**), CON (**j**), Consolation (**k**) and Aggression (**l**). Scale bars, 100 μm. The enlarged views of the selected boxed areas (300 μm × 300 μm) , and co-labeling neurons were characterized by white arrows. Scale bars, 50 μm. n = 3 voles / group. **m**, **n** Distinction of co-labeled c-Fos and fluorescent tracer ratio between AAV (2/1) system and CAG-mWGA strategy in the AI^{MeA} (**m**) and $VMHvl^{MeA}$ (**n**). In (**m**), AAV1-CON versus mWGA-CON, $p = 0.2535$; AAV1-Consolation versus mWGA-Consolation, $p = 0.4714$; AAV1-Aggression versus mWGA-Aggression, $p = 0.0869$; AAV1-Separation versus mWGA-Separation, $p = 0.2082$. In (**n**), AAV1-CON versus mWGA-CON, $p = 0.7781$; AAV1-Consolation versus mWGA-Consolation, $p = 0.8594$; AAV1-Aggression versus mWGA-Aggression, $p = 0.8119$; AAV1-Separation versus mWGA-Separation, $p = 0.3910$. $^{****}p < 0.0001$. Data analyzed by One-way ANOVA with Sidak's multiple comparison test (**c**, **d**) and 2-tail unpaired t-test (**m**, **n**). Data are presented as the means +/- SEM. Statistical details are presented in Supplementary Data. 1 file. Source data are provided as a Source Data file.

Supplementary Fig. 8

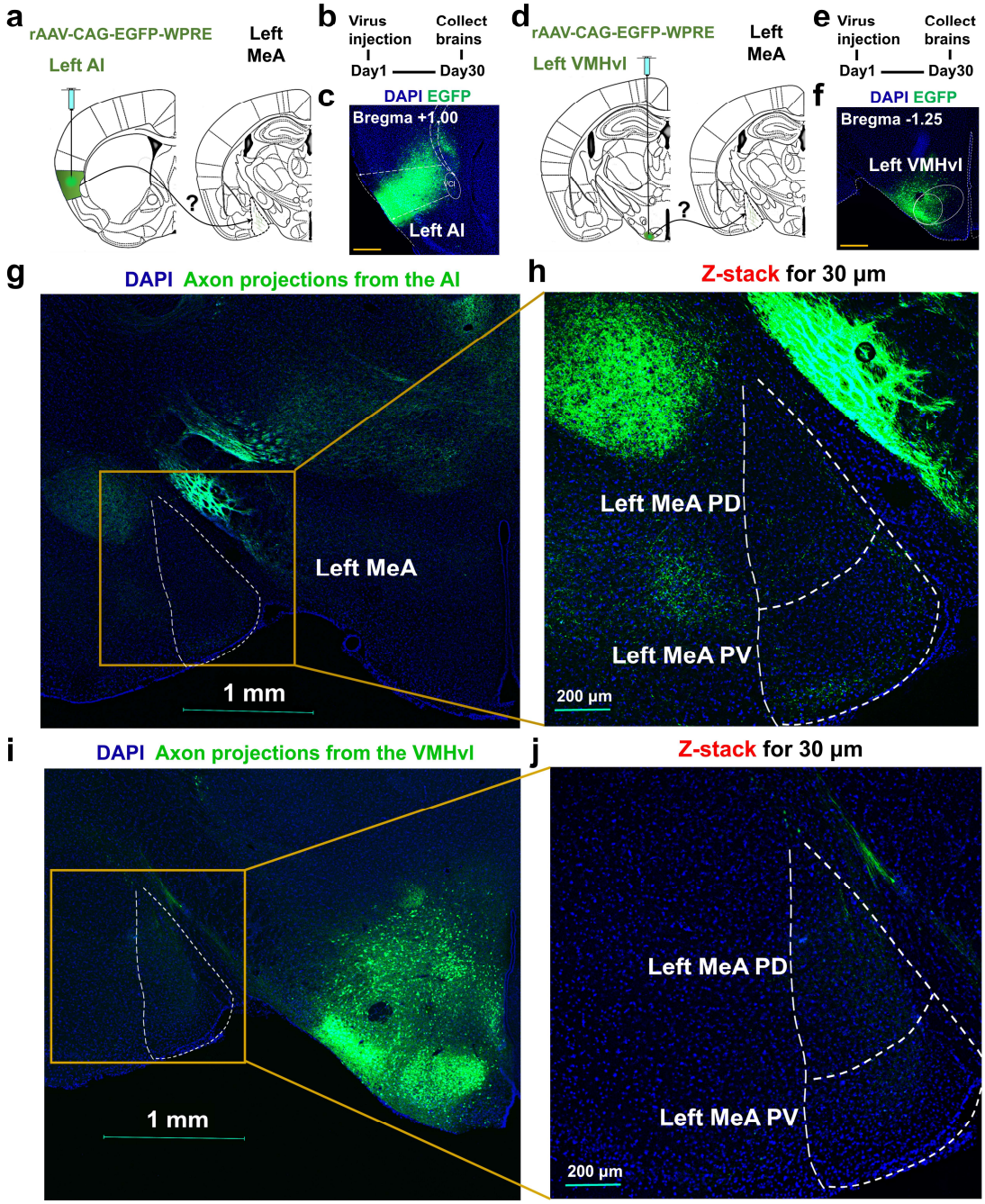

Supplementary Fig. 8 | Confirmation the rare existence of axonal projections to the MeA from the AI and VMHvl using AAV2/9-type anterograde virus carrying EGFP florescence, respectively.

a–**f** Diagram showing virus injection regimen (adapted from *The Mouse Brain in Stereotaxic Coordinates* by Paxinos and Franklin, **a**, **d**), schedule (**b**, **e**) and representative images of rAAV injection site (**c**, **f**). 3 independent repetitions with similar results in (**c**, **f**). Scale bars, 500 μm. **g**–**j** Representative 30μm Z-stack images of axonal fibers (EGFP, green) to the MeA from the AI and VMHvl. Scale bars, 1000 μm (**g**, **i**) and 200 μm (**h**, **j**).

Supplementary Fig. 9

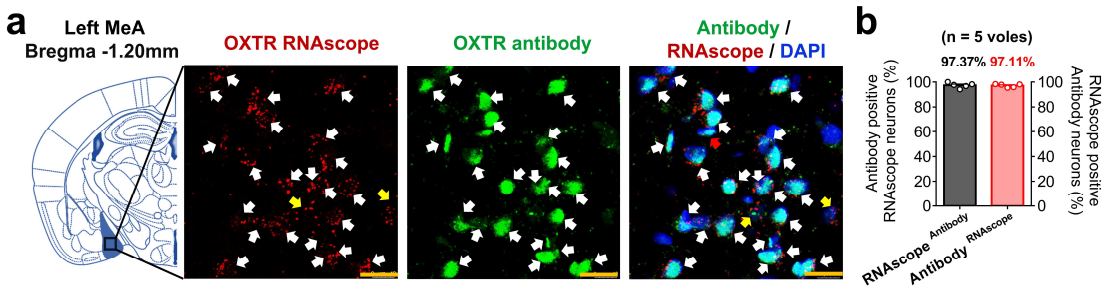

Supplementary Fig. 9 | The validation of the efficiency and specificity of OXTR antibody by RNAscope Multiplex Fluorescent v2 Assay combined with Immunofluorescence–Integrated Co-detection Workflow (ICW).

a Representative co-labeled images of OXTR RNAscope (AF570, red) and OXTR antibody (AF488, green) (adapted from *The Mouse Brain in Stereotaxic Coordinates* by Paxinos and Franklin). Co-labeling neurons were characterized by white arrows. The neurons labeled by antibody but not by RNAscope were characterized by red arrows. The neurons labeled by RNAscope but not by antibody were characterized by yellow arrows. Scale bars, 15 μm. **b** Percentage of co-labeling neurons in antibody positive neurons and in RNAscope positive neurons, respectively (n = 5 voles). Data are presented as the means +/- SEM. Source data are provided as a Source Data file.

Supplementary Fig. 10

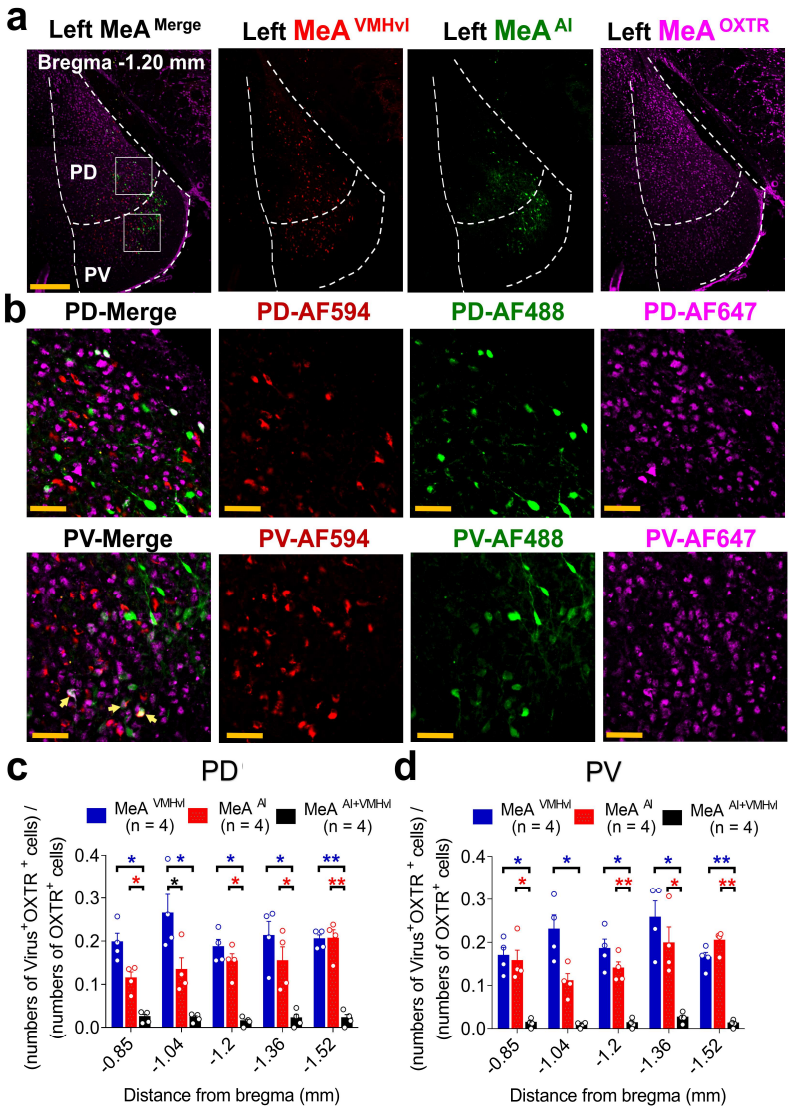

Supplementary Fig. 10 | The corresponding individual channels' images from representative overlapped images of MeA$^{OXTR+AI+VMHvl}$ and the proportion of MeA^{AI}, MeA^{VMHvl}, MeA $^{AI+VMHvl}$ expressing OXTR along the anteroposterior axis at the PD and PV subregions.

a, **b** The enlarged views of the selected white boxed areas (200 μm × 200 μm) in (**b**). Scale bars, 200 μm in (**a**) and 50 μm in (**b**). **c**, **d** Proportion of different retrograde virus positive and overlapped neurons expressing OXTR along the anteroposterior axis of the MeA PD (**c**) and PV (**d**). At the PD subregion (**c**), MeA^{AI} versus MeA$^{AI+VMHvl}$, p = 0.0219, 0.0918, 0.0231, 0.0462 and 0.0044 at bregma -0.85, -1.04, -1.20, -1.36 and -1.50 mm respectively; MeA^{VMHvl} versus MeA$^{AI+VMHvl}$, p = 0.0198, 0.0405, 0.0126, 0.0164 and 0.0073 at bregma -0.85, -1.04, -1.20, -1.36 and -1.50 mm respectively; MeA^{AI} versus MeA^{VMHvl}, p = 0.0174 at bregma -1.04. At the PV subregion (**d**), MeA^{AI} versus MeA$^{AI+VMHvl}$, p = 0.0337, 0.0518, 0.0056, 0.0411 and 0.0024 at bregma -0.85, -1.04, -1.20, -1.36 and -1.50 mm respectively; MeA^{VMHvl} versus MeA$^{AI+VMHvl}$, p = 0.0181, 0.0193, 0.0222, 0.0210 and 0.0074 at bregma -0.85, -1.04, -1.20, -1.36 and -1.50 mm respectively. $^{**}p < 0.01$, $^{*}p < 0.05$. Data analyzed by Repeated measure two-way ANOVA with Sidak's multiple comparison test (**c**, **d**). Data are presented as the means +/- SEM. Statistical details are presented in Supplementary Data. 1 file. Source data are provided as a Source Data file.

Supplementary Fig. 11

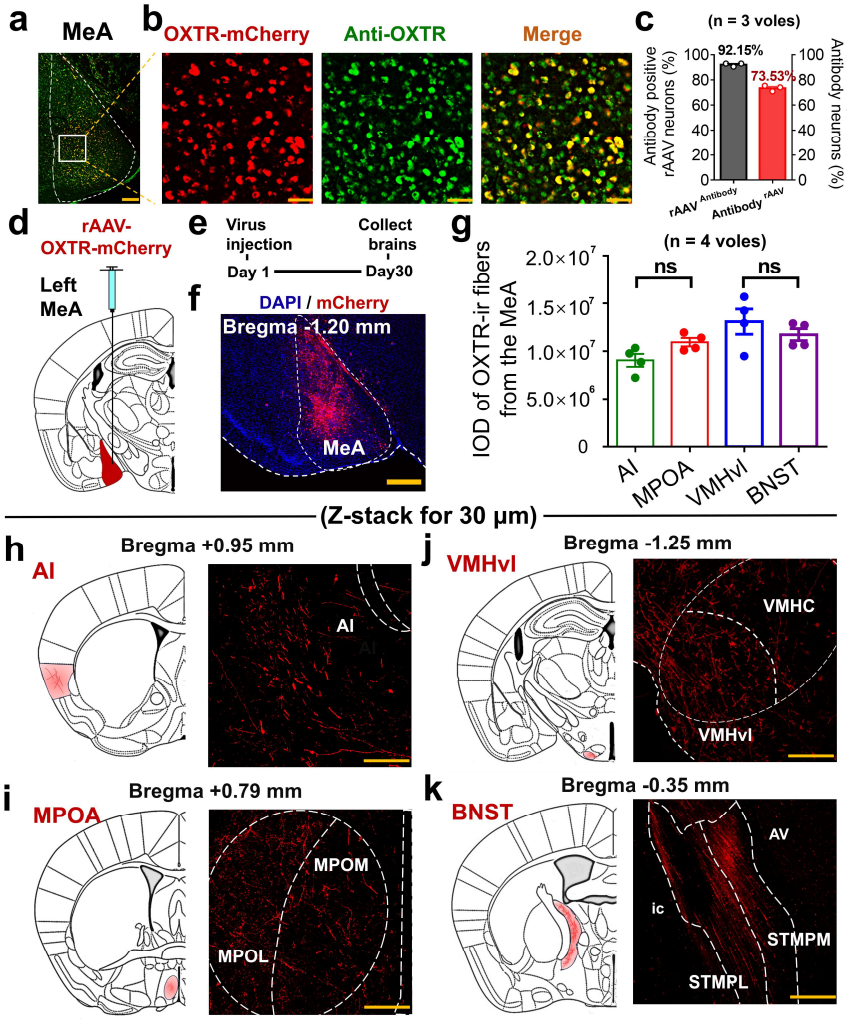

Supplementary Fig. 11 | Quantification of density of OXTR-ir fibers in the AI, MPOA, VMHvl and BNST after verification of transfection efficiency of rAAV-OXTR-mCherry by OXTR antibody.

a, **b** Overlapped images of neurons infected by rAAV-OXTR-mCherry (red) and neurons stained by OXTR antibody (AF488, green) (**a**). The enlarged views of the selected white boxed areas (300 μm × 300 μm) (**b**). Scale bars, 200 μm (**a**) and 50 μm (**b**). **c** Quantification of percentage of antibody-staining infective OXTR-mCherry neurons and OXTR-mCherry expressing antibody-staining neurons. n = 3 voles. **d**–**f** Diagram showing virus injection regimen (**d**), schedule (**e**) and representative images of rAAV injection site (**f**). 4 independent repetitions with similar results in (**f**). Scale bars, 500 μm. **g** Differences in IOD of OXTR-ir fibers (mCherry, red) between the AI, MPOA, VMHvl and BNST. n = 4 voles. AI versus MPOA, $p = 0.378$; VMHvl versus BNST, $p = 0.982$. **h**–**k** Representative 30 μm Z-stack images of OXTR-ir fibers (mCherry) in the AI (**h**), MPOA (**i**), VMHvl (**j**) and BNST (**k**). Scale bars, 100 μm. Diagrams were adapted from *The Mouse Brain in Stereotaxic Coordinates* by Paxinos and Franklin in (**d**, **h**, **i**, **j**, **k**). Data analyzed by Repeated measure one-way ANOVA with Sidak's multiple comparison test (**g**). Data are presented as the means +/- SEM. Statistical details are presented in Supplementary Data. 1 file. Source data are provided as a Source Data file. ns = no significance, IOD = integrated optical density, MPOA = medial preoptic area, BNST = bed nucleus of the stria terminalis.

Supplementary Fig. 12

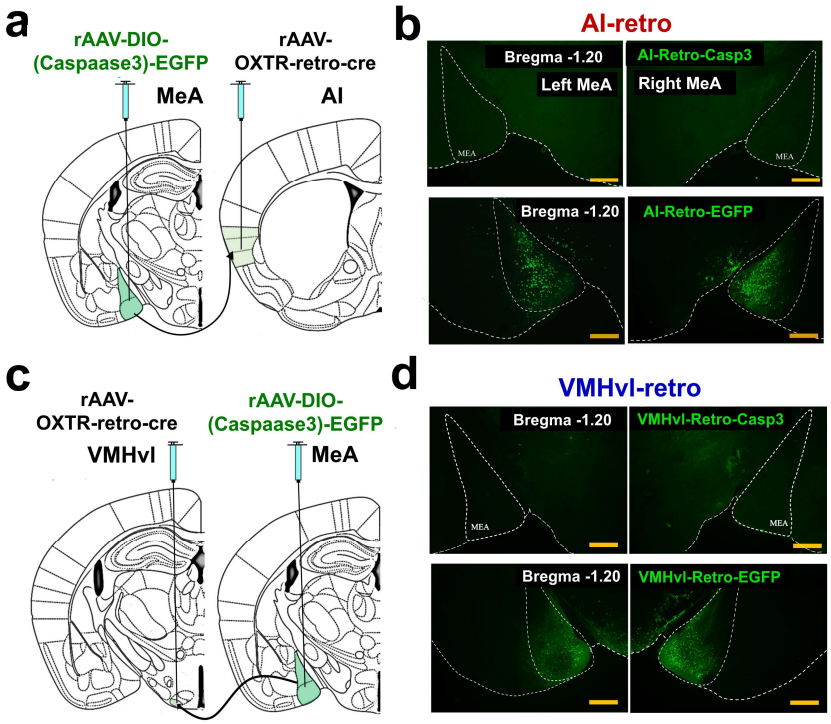

Supplementary Fig. 12 | Diagram showing protocol of virus injection for apoptosis experiment and representative images of bilateral Casp3-EGFP and EGFP expression (green) in the MeA$^{OXTR+AI}$ and MeA$^{OXTR+VMHvl}$.

7 independent repetitions with similar results in (**b**, **d**). Scale bars, 500 μm. Diagrams were adapted from *The Mouse Brain in Stereotaxic Coordinates* by Paxinos and Franklin in (**a**, **c**).

Supplementary Fig. 13

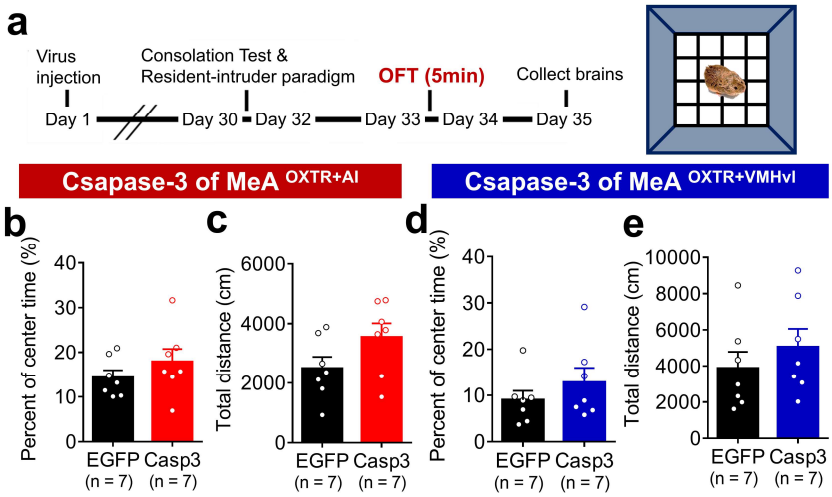

Supplementary Fig. 13 | Effect of apoptosis of the MeA$^{OXTR+AI}$ or MeA$^{OXTR+VMHvl}$ on locomotion and anxiety level.

a Schedule showing behavioral tests and a diagram of the open field test (OFT). **b**–**e** Behavioral performance caused by apoptosis of the MeA$^{OXTR+AI}$ and MeA$^{OXTR+VMHvl}$ respectively during OFT, n = 7 voles / group. Percentage of time spent in the center between the EGFP and Casp3 groups (**b**, **d**). Quantification of total distance between the two groups (**c**, **e**). In (**b**), p = 0.3055; In (**c**), p = 0.1098; In (**d**), p = 0.3283; In (**e**), p = 0.4030. Data analyzed by 2-tail unpaired t-test (**b**–**e**). Data are presented as the means +/- SEM. Statistical details are presented in Supplementary Data. 1 file. Source data are provided as a Source Data file.

Supplementary Fig. 14

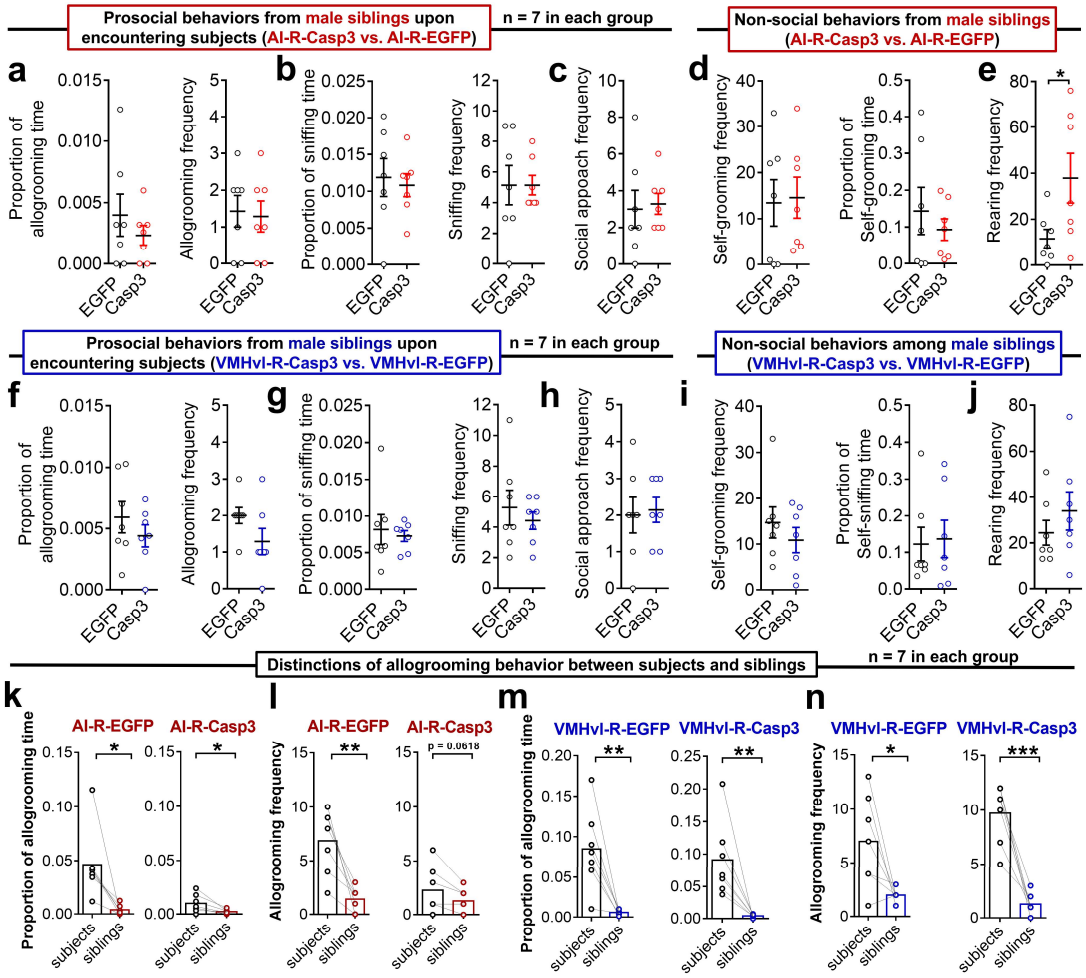

Supplementary Fig. 14 | Prosocial and non-social behavioral performance from the male stressed siblings upon encountering subjects in consolation test in the apoptosis experiment. **a**–**c**, **f**–**h** Quantitative distinction of duration proportion and frequency of allogrooming and sniffing, and frequency of social approach from male siblings between the AI-retro EGFP and Csap3 groups (**a**–**c**) or between the VMHvl-retro EGFP and Csap3 groups (**f**–**h**). p = 0.4027, = 0.8160, = 0.7337, > 0.9999, = 0.8111 in (**a**–**c**); p = 0.3494, 0.1152, 0.6914, 0.5167, 0.8142 in (**f**–**h**). **d**, **e**, **i**, **j** Quantitative distinction of duration proportion and frequency of self-grooming, and frequency of rearing from male siblings between the AI-retro EGFP and Csap3 groups (**d**, **e**), or between the VMHvl-retro EGFP and Csap3 groups (**i**, **j**). p = 0.8679, 0.4880, 0.4515 in (**d**, **e**), p = 0.3948, 0.8403, 0.3586 in (**i**, **j**). **k**–**n** Quantitative distinction of duration proportion and frequency of allogrooming between male siblings and subjects in the AI-retro EGFP, AI-retro Casp3, VMHvl-retro EGFP and VMHvl-retro Casp3 groups. p = 0.0151 and 0.0299 in (**k**); p = 0.0033 and 0.0618 in (**l**); p = 0.0052 and 0.0086 in (**m**); p = 0.0278 and 0.0004 in (**n**). $^{***}p < 0.001$, $^{**}p < 0.01$, $^{*}p < 0.05$. Data analyzed by 2-tail unpaired t-test (**a**–**j**) and 2-tail paired t-test (**k**–**n**). Data are presented as the means +/- SEM. Statistical details are presented in Supplementary Data. 1 file. Source data are provided as a Source Data file.

Supplementary Fig. 15

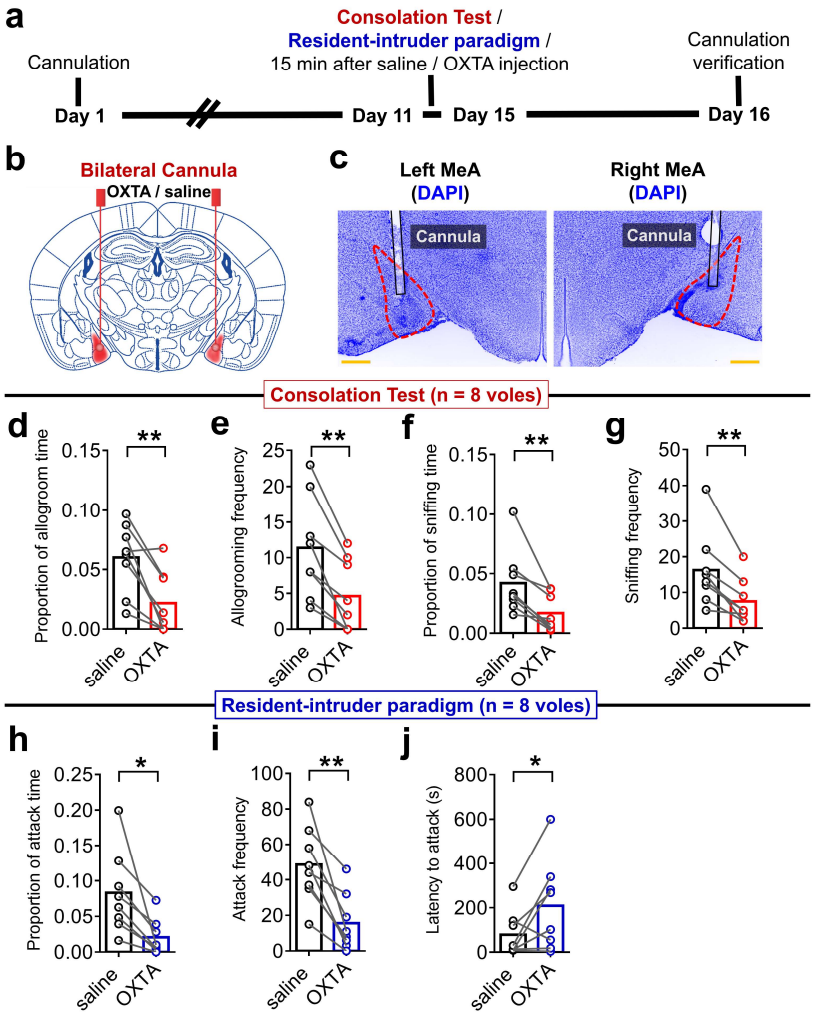

Supplementary Fig. 15 | The effect of microinjection of OXTR antagonists (OXTA) in the bilateral MeA on consolation and aggression behaviors.

a–**c** Diagram showing experimental schedule (**a**), schematic representation of MeA infusion sites (adapted from *The Mouse Brain in Stereotaxic Coordinates* by Paxinos and Franklin, **b**) and representative photomicrograph of the injection site (**c**). 8 independent repetitions with similar results. Scale bars, 500 μm. **d**–**g** Quantitative distinction of duration proportion and frequency of allogrooming and sniffing between the saline and OTA groups. $p = 0.0041, 0.0012, 0.0055, 0.0023$ in (**d**–**g**). **h**–**j** Quantitative distinction of duration proportion and frequency of attack, and latency to attack between the saline and OXTA groups. $p = 0.0132, 0.0021, 0.0483$ in (**h**–**j**). n = 8 voles in (**d**–**j**). $^{**}p < 0.01$, $^{*}p < 0.05$. Data analyzed by 2-tail paired t-test (**d**–**j**). Data are presented as the means +/- SEM. Statistical details are presented in Supplementary Data. 1 file. Source data are provided as a Source Data file. OXTA = OXTR antagonist ([d (CH2) 51, Tyr (Me) 2, Thr4, Orn8, des-Gly-NH29]-Vasotocin trifluoroacetate salt) (0.5 ng / 200 nl per side).

Supplementary Fig. 16

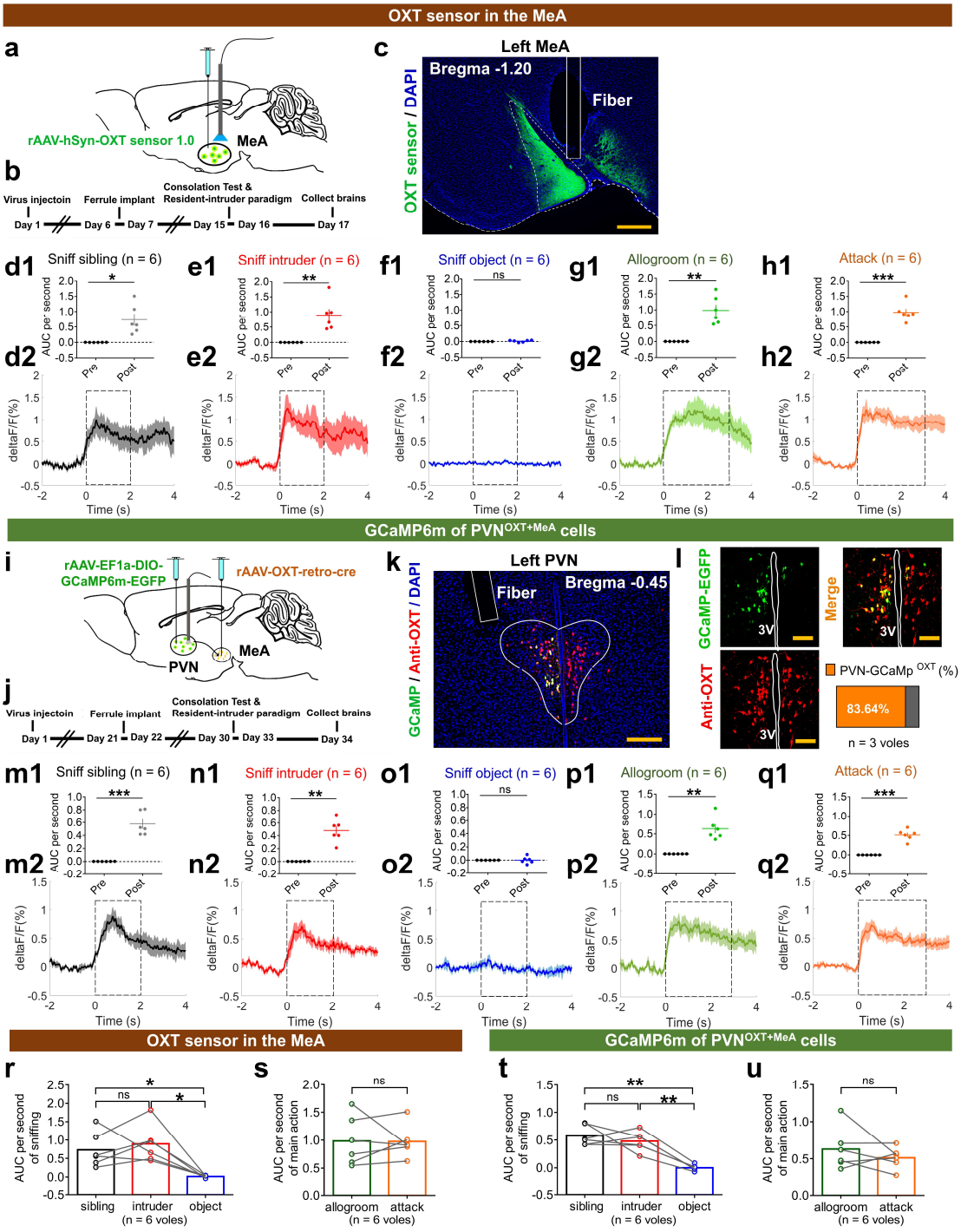

Supplementary Fig. 16 | Dynamic changes of fluorescence signal in MeA$^{OXT\ sensor}$ and PVN$^{OXT+MeA}$ during various social behaviors.

a, **b**, **i**, **j** Virus regimen (adapted from *The Mouse Brain in Stereotaxic Coordinates* by Paxinos and Franklin, **a**, **i**) and schedule (**b**, **j**) for calcium signal recording. **c**, **k** Images of OXT sensor (green) and GCaMP6m (green) in the MeA and PVN$^{OXT+MeA}$. Scale bars, 500 μm (**c**) and 200 μm (**k**). 6 independent repetitions with similar results in (**c**) and (**k**). **l** Overlapped images of of OXT-GCaMP6m and anti-OXT (Cy3, red). Scale bars, 100 μm; n = 3 voles. **d1**–**h1**, **m1**–**q1** Changes of fluorescent signals in the MeA$^{OXT\ sensor}$ and PVN$^{OXT+MeA}$ before and after sniffing siblings (**d1**, *p* =

0.013; **m1**, $p < 0.001$), intruder (**e1**, $p < 0.010$; **n1**, $p < 0.010$), object (**f1**, **o1**), and allogrooming (**g1**, $p < 0.010$; **p1**, $p < 0.010$) and attacking (**h1**, $p < 0.001$; **q1**, $p < 0.001$). **d2**–**h2**, **m2**–**q2** Peri-event plot of the representative signal (delta F/F, %) in the $MeA^{OXT\ sensor}$ and $PVN^{OXT+MeA}$ aligned to onsets of various social behaviors. Colored lines indicate group averages of 6-s calcium signal and shaded areas indicate S.E.M. Dotted boxes define time windows for analyzing AUC per second of single event. **r**–**u** AUC per second distinctions of fluorescent signal traces during different social behaviors in the $MeA^{OXT\ sensor}$ (**r**, **s**) and $PVN^{OXT+MeA}$ (**t**, **u**). Signals of $MeA^{OXT\ sensor}$: sniffing sibling versus intruder, $p = 0.892$; sniffing sibling versus object, $p = 0.045$; sniffing intruder versus object, $p = 0.023$. Signals of $PVN^{OXT+MeA}$: sniffing sibling versus intruder, $p = 0.821$; sniffing sibling versus object, $p = 0.004$; sniffing intruder versus object, $p = 0.001$. n = 6 and 6 voles for calcium signal of $PVN^{OXT+MeA}$ and $MeA^{OXT\ sensor}$, respectively. Data analyzed by 2-tail paired t-test (**d1**–**h1**, **m1**–**q1**, **s**, **u**) and Repeated measure one-way ANOVA with Sidak's multiple comparison test (**r**, **t**). $^{***}p < 0.001$, $^{**}p < 0.01$, $^{*}p < 0.05$. Data are presented as the means +/- SEM. Statistical details are presented in Supplementary Data. 1 file. Source data are provided as a Source Data file. AUC = area under curve; Delta F/F (%) = change in fluorescence as a function of baseline fluorescence; ns = no significance.

Supplementary Fig. 17

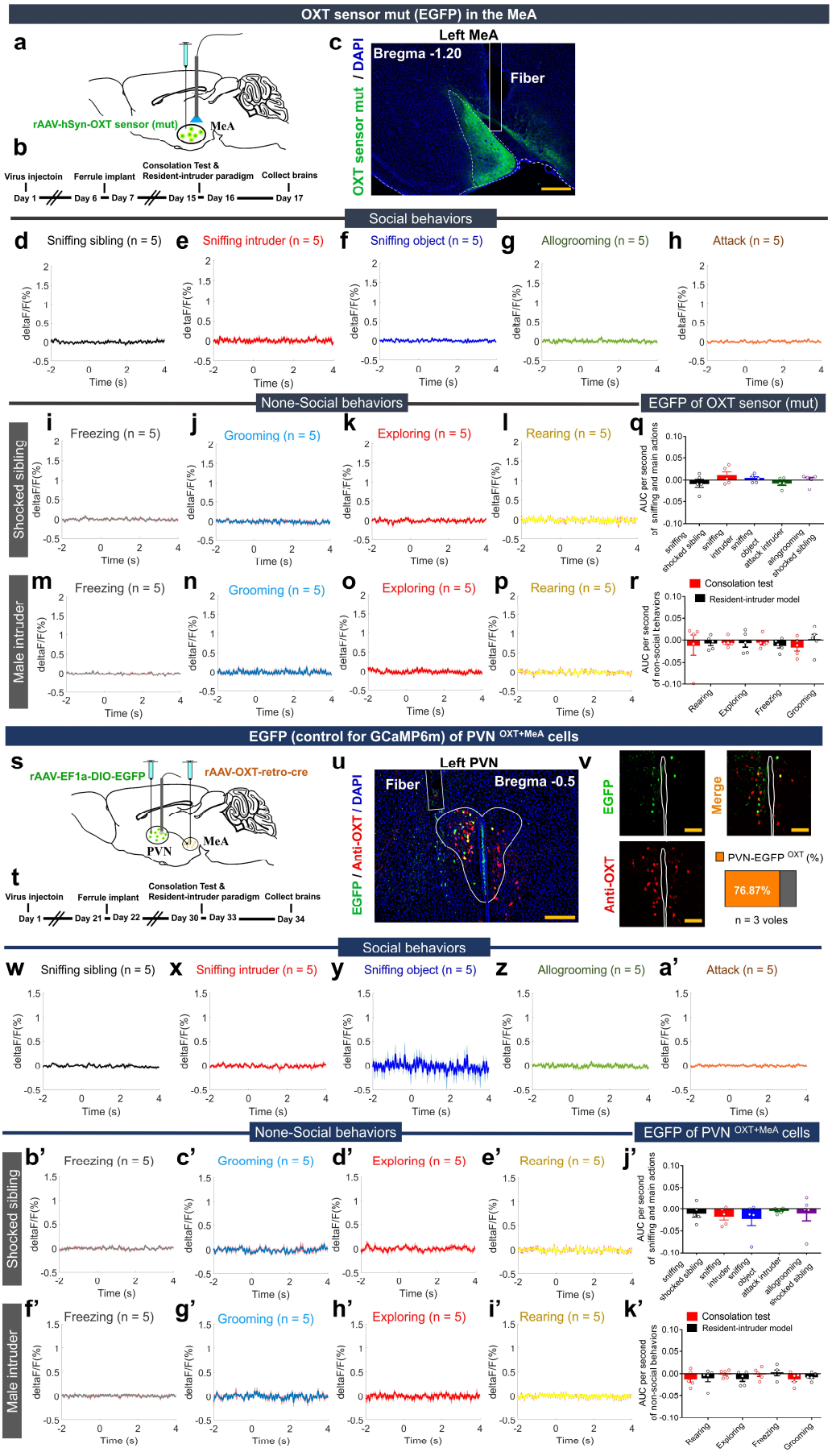

Supplementary Fig. 17 | Dynamics of EFGP-fluorescence signal in MeA$^{\text{OXT sensor (mut)}}$ and PVN$^{\text{OXT+MeA}}$ during various social and non-social behaviors.

a, **b**, **s**, **t** Virus regimen (adapted from *The Mouse Brain in Stereotaxic Coordinates* by Paxinos and Franklin, **a**, **s**) and schedule (**b**, **t**) for EFGP-fluorescence signal recording of the MeA$^{\text{OXT sensor (mut)}}$ and PVN$^{\text{OXT+MeA}}$. **c**, **u** Images of EGFP (green) expression in the MeA$^{\text{OXT sensor (mut)}}$ and PVN$^{\text{OXT+MeA}}$. Scale bars, 500 μm (**c**) and 200 μm (**u**). 5 independent repetitions with similar results in (**c**) and (**u**). **v** Overlapped images of OXT-EGFP and anti-OXT (Cy3, red). Scale bars, 100 μm; n = 3 voles. **d**–**p** Peri-event plot of the representative OXT sensor (mut) signal (delta F/F, %) in the MeA aligned to onsets of various social (**d**–**h**) and non-social behaviors (**i**–**p**). Colored lines indicate group averages of 6-s calcium signal and shaded areas indicate S.E.M. **q**, **r** AUC per second distinctions of OXT sensor (mut)-fluorescence traces during different social behaviors and non-social behaviors in the MeA. n = 5 voles in (**d**–**r**). **w**–**i'** Peri-event plot of the representative EGFP-PVN$^{\text{OXT+MeA}}$ signal (delta F/F, %) aligned to onsets of various social (**w**–**a'**) and non-social behaviors (**b'**–**i'**). **j'**, **k'** AUC per second distinctions of EGFP-PVN$^{\text{OXT+MeA}}$-fluorescence traces during different social behaviors (**j'**) and non-social behaviors (**k'**). n = 5 voles in (**u**–**j'**). Data analyzed by Repeated measure one-way ANOVA with Sidak's multiple comparison test (**q**, **r**, **j'**, **k'**). Data are presented as the means +/- SEM. Statistical details are presented in Supplementary Data. 1 file. Source data are provided as a Source Data file. AUC = area under curve; Delta F/F (%) = change in fluorescence as a function of baseline fluorescence.

Supplementary Fig. 18

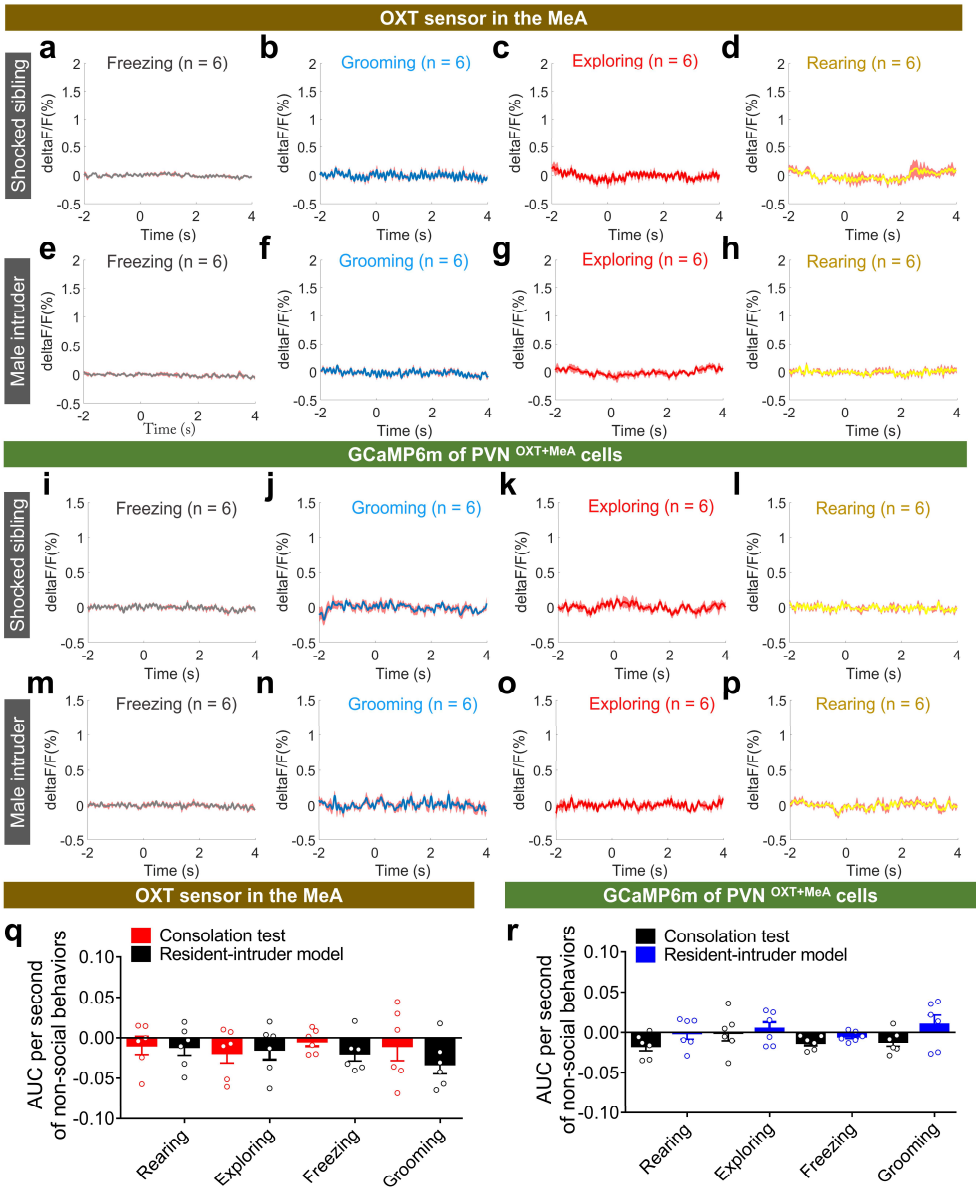

Supplementary Fig. 18 | Dynamics of fluorescence signal in the MeA$^{OXT\ sensor}$ and PVN$^{OXT+MeA}$ during various non-social behaviors.

a–**h** Peri-event plot of the representative fluorescent signal (delta F/F, %) in the MeA$^{OXT\ sensor}$ aligned to onsets of various non-social behaviors when meeting with the stressed siblings (**a**–**d**) and male intruders (**e**–**h**). **i**–**p** Peri-event plot of the representative calcium signal (delta F/F, %) in the PVN$^{OXT+MeA}$ aligned to onsets of various non-social behaviors when meeting with the stressed siblings (**i**–**l**) and male intruders (**m**–**p**). Colored lines indicate group averages of 6-s calcium signal and shaded areas indicate S.E.M. **q**, **r** AUC per second distinctions of calcium signal traces during different non-social behaviors in the MeA$^{OXT\ sensor}$ and PVN$^{OXT+MeA}$. 6 voles' fluorescent signal traces were collected and averaged (**a**–**h**, **q**); 6 calcium signal traces were collected and averaged (**i**–**p**, **r**). Data analyzed by Repeated measure one-way ANOVA with Sidak's multiple comparison test (**q**, **r**). Data are presented as the means +/- SEM. Statistical details are presented in Supplementary Data. 1 file. Source data are provided as a Source Data file. AUC = area under curve; Delta F/F (%) = change in fluorescence as a function of baseline fluorescence.

Supplementary Fig. 19

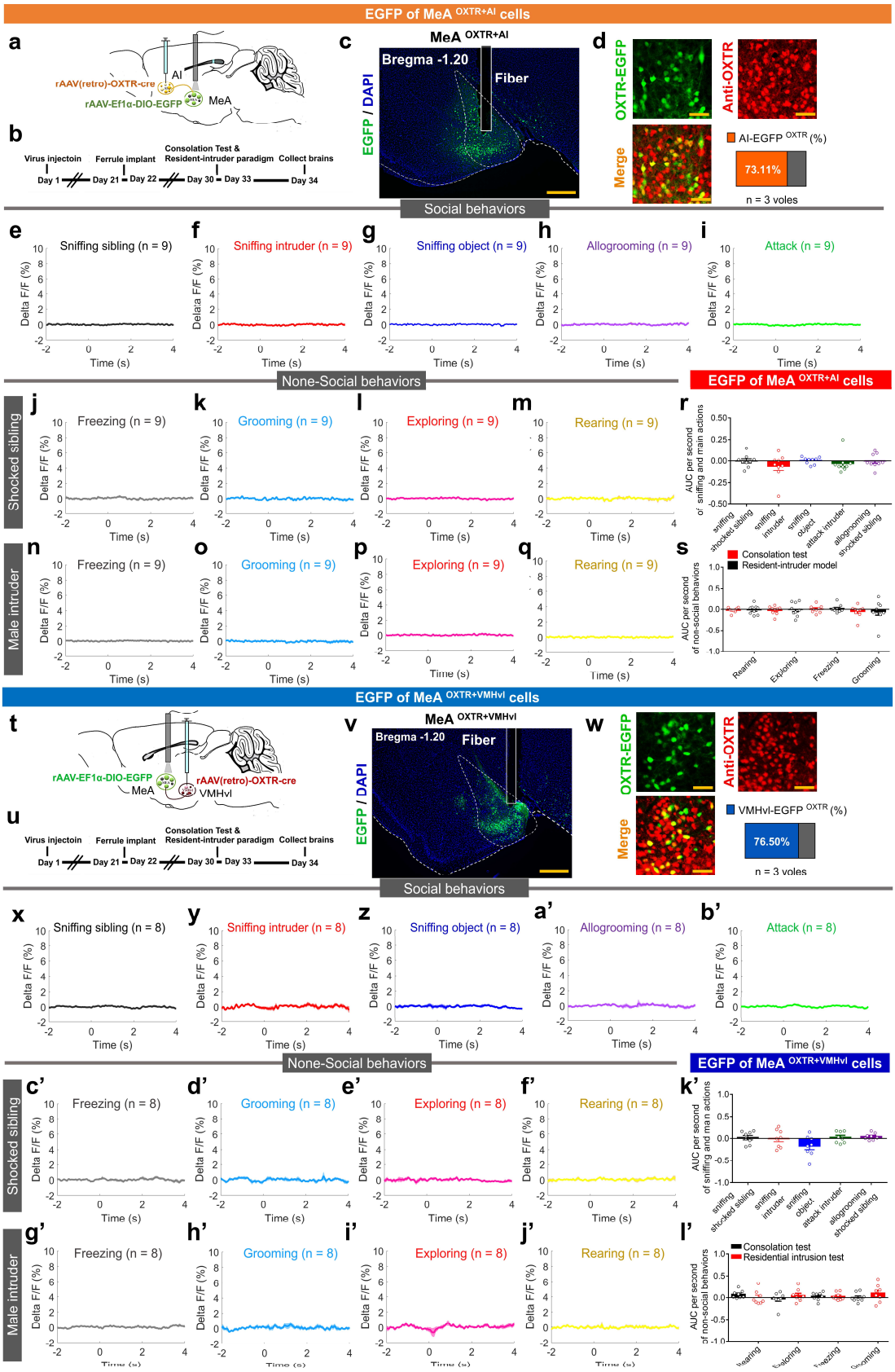

Supplementary Fig. 19 | Dynamics of EFGP-fluorescence signal in MeA$^{OXTR+AI}$ and MeA$^{OXTR+VMHvl}$ during various social and non-social behaviors.

a, **b**, **t**, **u** Virus regimen (adapted from *The Mouse Brain in Stereotaxic Coordinates* by Paxinos and Franklin, **a**, **t**) and schedule (**b**, **u**) for EFGP-fluorescence signal recording of the $MeA^{OXTR+AI}$ and $MeA^{OXTR+VMHvl}$. **c**, **v** Images of EGFP (green) expression in the $MeA^{OXTR+AI}$ and $MeA^{OXTR+VMHvl}$. Scale bars, 500 μm. 9 and 8 independent repetitions with similar results in (**c**) and (**v**). **d**, **w** Overlapped images of OXTR-EGFP and OXTR (Cy3, red) in the $MeA^{OXTR+AI}$ (**c**) and $MeA^{OXTR+VMHvl}$ (**u**), Scale bars, 50 μm; n = 3 voles / group. **e**–**q** Peri-event plot of the representative EFGP-fluorescence signal (Delta F/F, %) in the $MeA^{OXTR+AI}$ aligned to onsets of various social (**e**–**i**) and non-social behaviors (**j**–**q**). Colored lines indicate group averages of 6-s calcium signal and shaded areas indicate S.E.M. **r**, **s** AUC per second distinctions of EFGP-fluorescence traces during different social behaviors and non-social behaviors in the $MeA^{OXTR+AI}$. n = 9 voles in (**e**–**s**). **x**–**l'** Peri-event plot of the representative EFGP-fluorescence signal (Delta F/F, %) in the $MeA^{OXTR+VMHvl}$ aligned to onsets of various social (**x**–**b'**) and non-social behaviors (**c'**–**j'**). **k'**, **l'** AUC per second distinctions of EFGP-fluorescence traces during different social behaviors (**k'**) and non-social behaviors (**l'**) in the $MeA^{OXTR+VMHvl}$. n = 8 voles (**x**–**l'**). No any distinctions were found. Data analyzed by Repeated measure one-way ANOVA with Sidak's multiple comparison test (**r**, **s**, **k'**, **l'**). Data are presented as the means +/- SEM. Statistical details are presented in Supplementary Data. 1 file. Source data are provided as a Source Data file. AUC = area under curve; Delta F/F (%) = change in fluorescence as a function of baseline fluorescence.

Supplementary Fig. 20

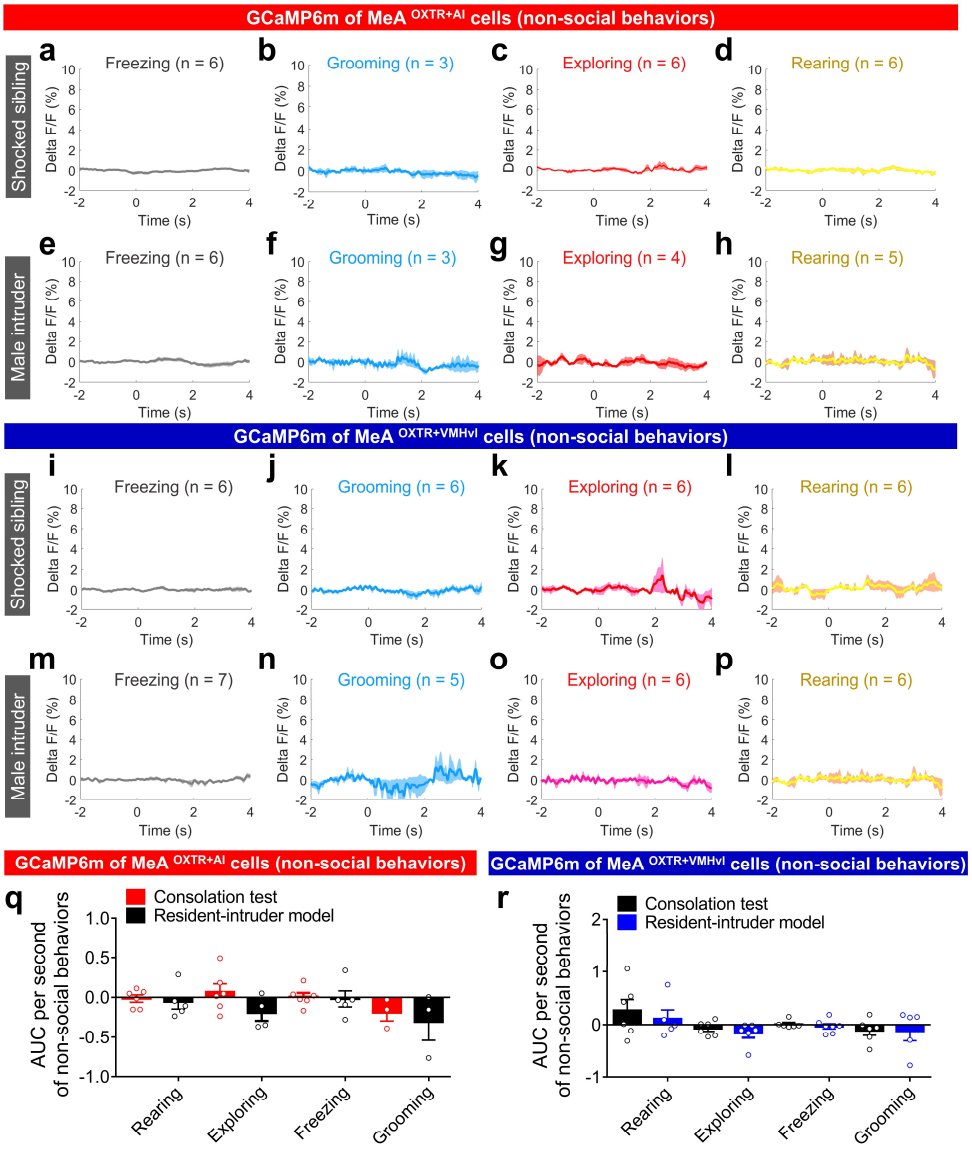

Supplementary Fig. 20 | Dynamics of GCaMP6m-fluorescence signal in the MeA$^{OXTR+AI}$ and MeA$^{OXTR+VMHvl}$ during various non-social behaviors.

a–**h** Peri-event plot of the representative calcium signal (Delta F/F, %) in the MeA$^{OXTR+AI}$ aligned to onsets of various non-social behaviors when meeting with the stressed siblings (**a**–**d**) and male intruders (**e**–**h**). **i**–**p** Peri-event plot of the representative calcium signal (Delta F/F, %) in the MeA$^{OXTR+VMHvl}$ aligned to onsets of various non-social behaviors when meeting with the stressed siblings (**i**–**l**) and male intruders (**m**–**p**). Colored lines indicate group averages of 6-s calcium signal and shaded areas indicate S.E.M. **q**, **r** AUC per second distinctions of calcium signal traces during different non-social behaviors in the MeA$^{OXTR+AI}$ and MeA$^{OXTR+VMHvl}$. n = 3–6 voles' calcium signal traces were collected and averaged (**a**–**h**, **q**); n = 5–7 voles' calcium signal traces were collected and averaged (**i**–**p**, **r**). No any distinctions were found. Data analyzed by One-way ANOVA with Sidak's multiple comparison test (**q**, **r**). Data are presented as the means +/- SEM. Statistical details are presented in Supplementary Data. 1 file. Source data are provided as a Source Data file. AUC = area under curve; Delta F/F (%) = change in fluorescence as a function of baseline fluorescence.

Supplementary Fig. 21

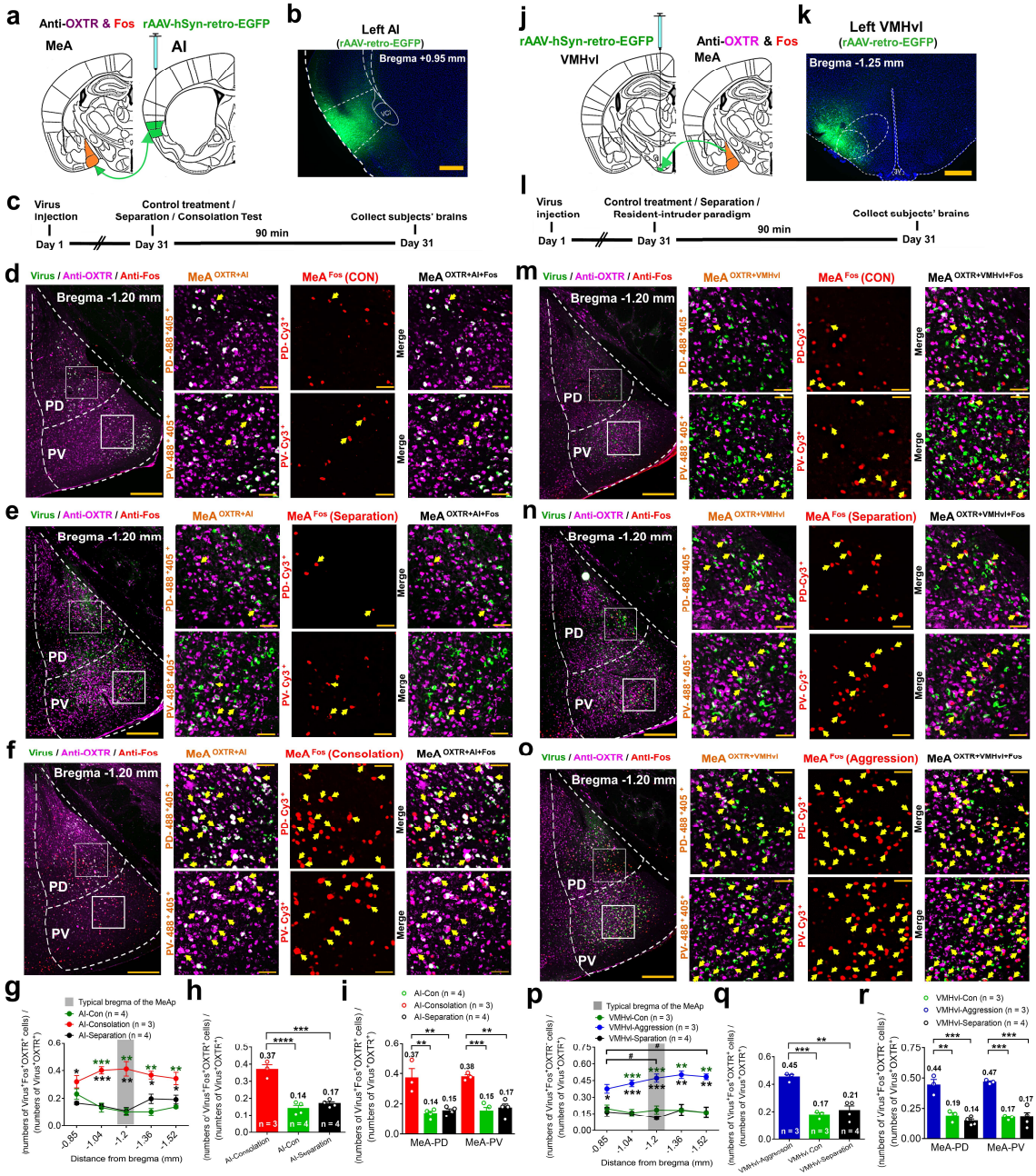

Supplementary Fig. 21 | Morphological analysis of association between the MeA$^{OXTR+AI}$ and consolation behavior, and between the MeA$^{OXTR+VMHvl}$ and aggression.

a, **c**, **j**, **l** Diagram showing retrograde AAVs injection regimen (adapted from *The Mouse Brain in Stereotaxic Coordinates* by Paxinos and Franklin, **a**, **j**) and schedule (**c**, **l**). **b**, **k** Representative images of rAAV-retro EGFP (green) injections sites at AI and VMHvl. Scale bars, 500 μm. 11 and 10 independent repetitions with similar results in (**b**) and (**k**). **d**–**f**, **m**–**o** Representative co-labeling images of AAVs tracing, anti OXTR (AF405, magenta) and anti c-Fos (Cy3, red) at PD and PV subregions among Con, Separation and Consolation groups, or among Con, Separation and Aggression groups (scale bars, 200 μm). The enlarged views of the selected boxed areas (300 μm × 300 μm) (scale bars, 50 μm). Merged neurons were characterized by yellow arrows. **g**, **p** Proportion of activated neurons in the total OXTR neurons retrograded from the AI and VMHvl, along the anteroposterior axis of the MeA. * and # implies between-group discrepancy at a same

site and intergroup discrepancy at different sites, respectively. **h**, **q** Proportion distinction of activated OXTR neurons retrograded from the AI between the Separation, Con and Consolation groups, or from the VMHvl between the Separation, Con and Aggression groups. **i**, **r** Proportion distinction of the triple-marked neurons in PD and PV after separation, control treatment and consolation test, or after the separation, control treatment and resident-intruder paradigm. In (**g**–**i**), AI-Separation (n = 4 voles), AI-Con (n = 4 voles) and AI-Consolation (n = 3 voles). In (**p**–**r**), VMHvl-Separation (n = 4 voles), VMHvl-Con (n = 3 voles) and VMHvl-Aggression (n = 3 voles). $^{****}p < 0.0001$, $^{***}p < 0.001$, $^{**}p < 0.01$, $^{*}p < 0.05$; $^{\#}p < 0.05$. Data analyzed by Repeated measure two-way ANOVA with Sidak's multiple comparison test (**g**, **i**, **p**, **r**) and One-way ANOVA with Sidak's multiple comparison test (**h**, **q**). Data are presented as the means +/- SEM. Statistical details are presented in Supplementary Data. 1 file. Source data are provided as a Source Data file.

Supplementary Fig. 22

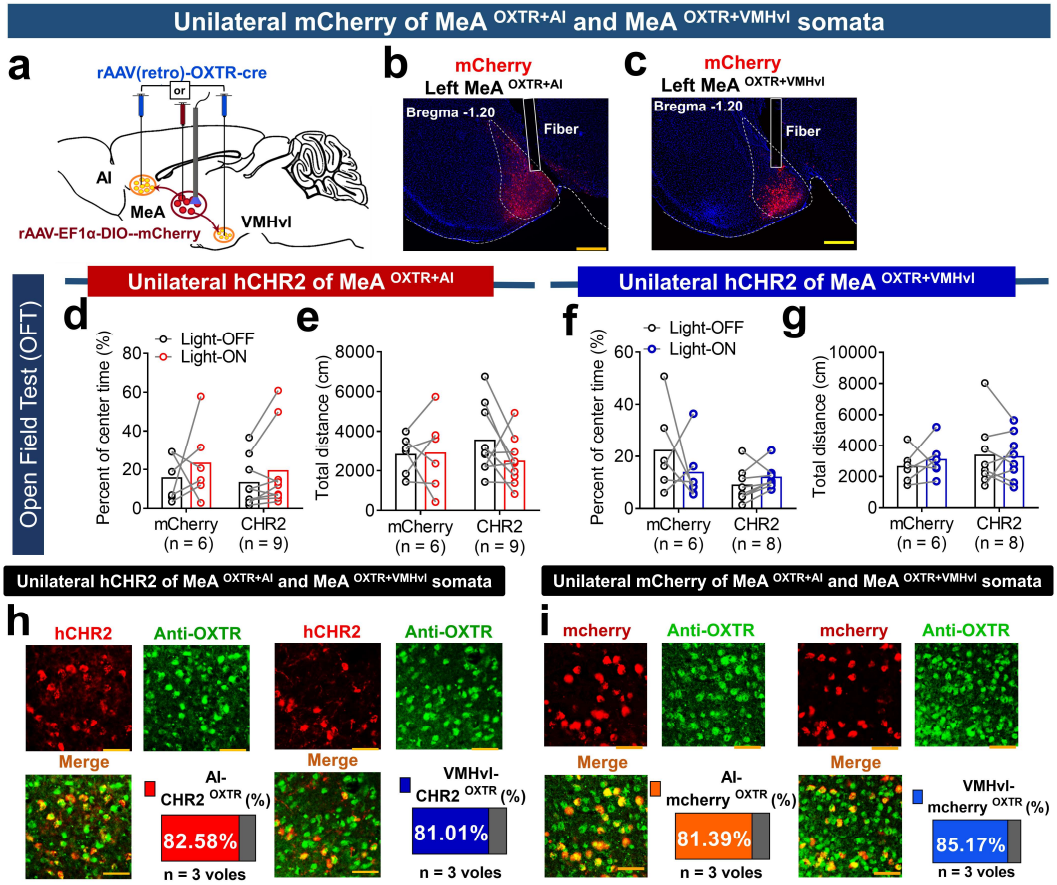

Supplementary Fig. 22 | Effects of optogenetic activation of somata of the MeA$^{OXTR+AI}$ and MeA$^{OXTR+VMHvl}$ on anxiety level and locomotion.

a Viral regimen for control experiment of CHR2 in somata of the MeA$^{OXTR+AI}$ and MeA$^{OXTR+VMHv}$. Diagram was adapted from *The Mouse Brain in Stereotaxic Coordinates* by Paxinos and Franklin. **b**, **c** Images of OXTR-mCherry (red) expression in the MeA$^{OXTR+AI}$ and MeA$^{OXTR+VMHvl}$. Scale bars, 500 μm. 6 independent repetitions with similar results in (**b**) and (**c**). **d**–**g** Behavioral distinction of percentage of center duration and total distance between the CHR2 and mCherry groups in MeA$^{OXTR+AI}$ somata (**d** and **e**), and MeA$^{OXTR+VMHvl}$ somata (**f** and **g**). n (mCherry) = 6 voles, n (CHR2) = 9 voles were used in CHR2 of the MeA$^{OXTR+AI}$ somata (**d** and **e**); n (mCherry) = 6 voles, n(CHR2) = 8 voles were used in CHR2 of the MeA$^{OXTR+VMHvl}$ somata (**f** and **g**). **h**, **i** The corresponding individual channels' images from representative overlapped images of hCHR2-MeA$^{OXTR+AI}$ and hCHR2-MeA$^{OXTR+VMHvl}$ somata (**h**), and overlapped images of mCherry-MeA$^{OXTR+AI}$ and mCherry-MeA$^{OXTR+VMHvl}$ somata (**i**). Scale bars, 50 μm. Data analyzed by Repeated measure two-way ANOVA with Sidak's multiple comparison test (**d**, **e**, **f**, **g**). Data are presented as the means +/- SEM. Statistical details are presented in Supplementary Data. 1 file. Source data are provided as a Source Data file.

Supplementary Fig. 23

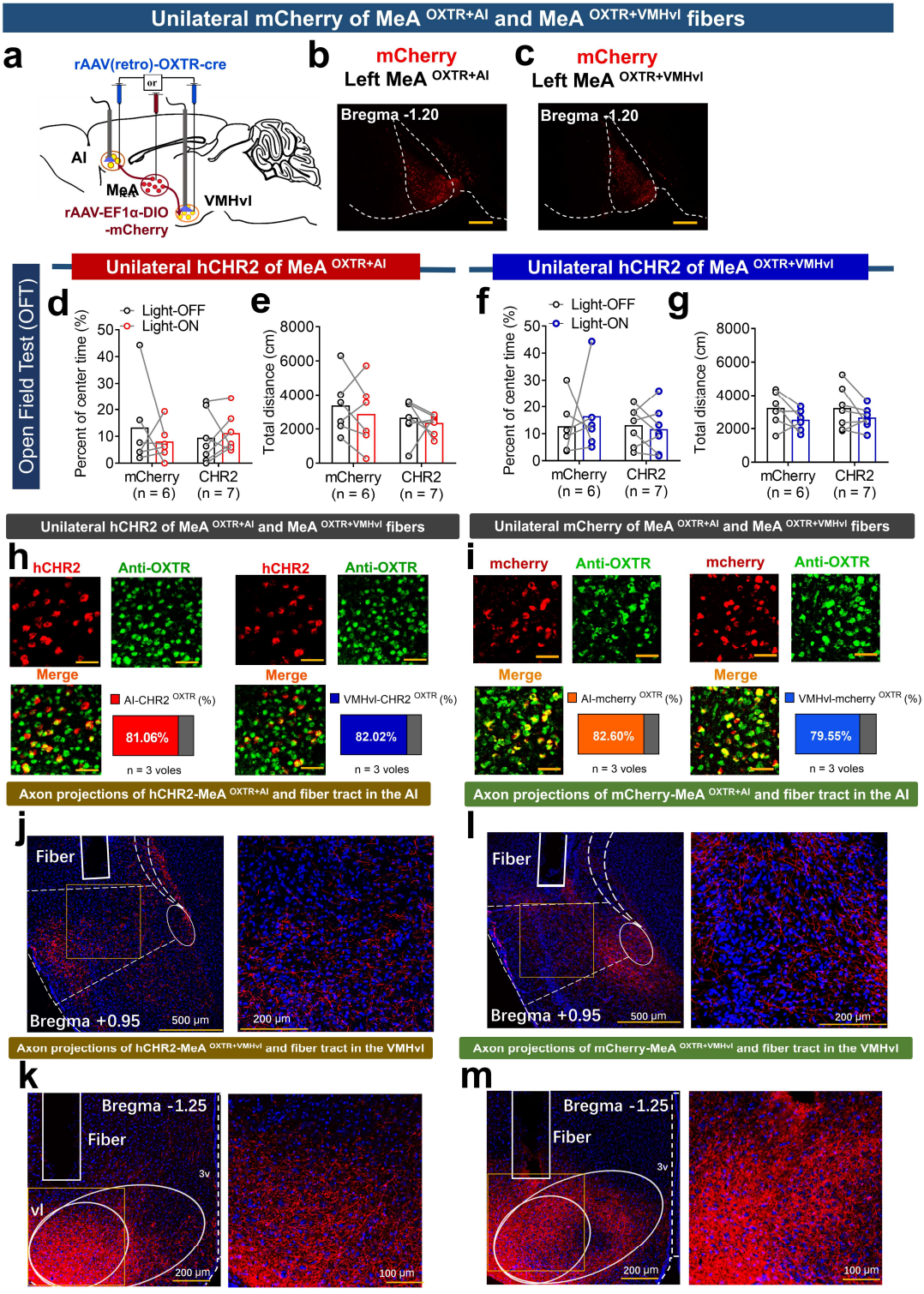

Supplementary Fig. 23 | Effects of optogenetic activation of fibers of the MeA$^{OXTR+AI}$ and MeA$^{OXTR+VMHvl}$ on anxiety level and locomotion.

a Viral regimen for control experiment of CHR2 in fibers of the MeA$^{OXTR+AI}$ and MeA$^{OXTR+VMHvl}$. Diagram was adapted from *The Mouse Brain in Stereotaxic Coordinates* by Paxinos and Franklin. **b**, **c** Images of OXTR-mCherry (red) expression in the MeA$^{OXTR+AI}$ and MeA$^{OXTR+VMHvl}$. Scale bars, 500 μm. 6 independent repetitions with similar results in (**b**) and (**c**). **d**–**g** Behavioral

distinction of percentage of center duration and total distance between the CHR2 and mCherry groups in $MeA^{OXTR+AI}$ fibers (**d**, **e**) and $MeA^{OXTR+VMHvl}$ fibers (**f**, **g**). n (mCherry) = 6 voles, n (CHR2) = 7 voles were used in CHR2 of the $MeA^{OXTR+AI}$ fibers (**d**, **e**); n (mCherry) = 6 voles, n(CHR2) = 7 voles were used in CHR2 of the $MeA^{OXTR+VMHvl}$ fibers (**f**, **g**). **h**, **i** Corresponding individual channels' images from representative overlapped images of hCHR2-$MeA^{OXTR+AI}$ somata and anti-OXTR cells and overlapped images of hCHR2-$MeA^{OXTR+VMHvl}$ somata and anti-OXTR cells, and overlapped images of mCherry-$MeA^{OXTR+AI}$ somata and anti-OXTR cells and overlapped images of mCherry-$MeA^{OXTR+VMHvl}$ somata and anti-OXTR cells. Scale bars, 50 μm. **j**, **k** Representative axon projections and fiber tract of hCHR2-$MeA^{OXTR+AI}$ and hCHR2-$MeA^{OXTR+VMHvl}$ in the AI and VMHvl. **l**, **m** Representative axon projections and fiber tract of mCherry-$MeA^{OXTR+AI}$ and $MeA^{OXTR+VMHvl}$ in the AI and VMHvl. Data analyzed by Repeated measure two-way ANOVA with Sidak's multiple comparison test (**d**, **e**, **f**, **g**). Data are presented as the means +/- SEM. Statistical details are presented in Supplementary Data. 1 file. Source data are provided as a Source Data file.

Supplementary Fig. 24

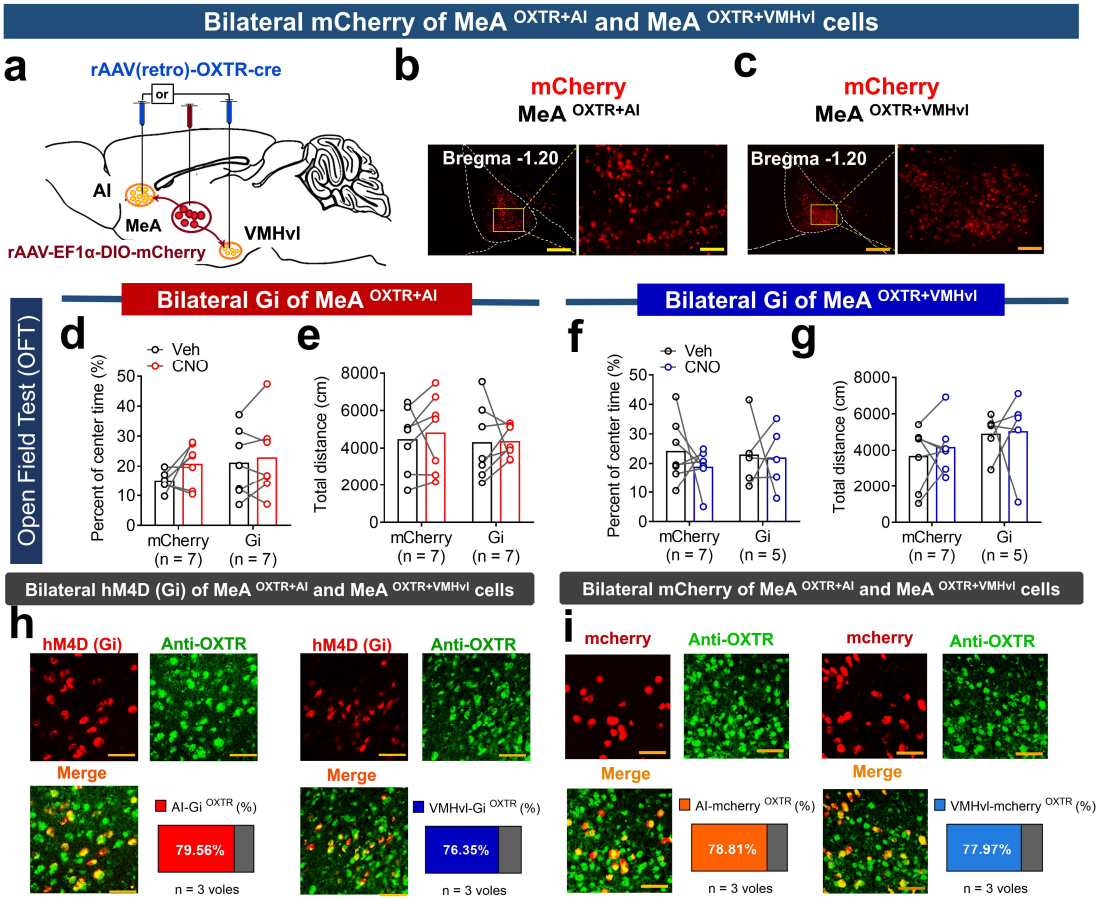

Supplementary Fig. 24 | Effects of pharmacogenetic inhibition of the MeA$^{OXTR+AI}$ and MeA$^{OXTR+VMHvl}$ on anxiety level and locomotion.

a Viral regimen for control experiments of hM4D (Gi) of the MeA$^{OXTR+AI}$ and MeA$^{OXTR+VMHvl}$. Diagram was adapted from *The Mouse Brain in Stereotaxic Coordinates* by Paxinos and Franklin. **b**, **c** Images of OXTR-mCherry expression (red) in the MeA$^{OXTR+AI}$ and MeA$^{OXTR+VMHvl}$. Scale bars, 500 μm (left) and 200 μm (right). 7 independent repetitions with similar results in (**b**) and (**c**). **d**–**g** Behavioral distinction of percent of center duration and total distance between the Gi and mCherry groups in the MeA$^{OXTR+AI}$ (**d**, **e**) and MeA$^{OXTR+VMHvl}$ (**f**, **g**). n (mCherry) = 7 voles, n (Gi) = 7 voles were used in the MeA$^{OXTR+AI}$ (**d**, **e**); n (mCherry) = 7 voles, n (Gi) = 5 voles were used in the MeA$^{OXTR+VMHvl}$ (**f**, **g**). **h**, **i** Corresponding individual channels' images from representative overlapped images of Gi-MeA$^{OXTR+AI}$ and Gi-MeA$^{OXTR+VMHvl}$ somata, and mCherry-MeA$^{OXTR+AI}$ and mCherry-MeA$^{OXTR+VMHvl}$ somata. Scale bars, 50 μm. Data analyzed by Repeated measure two-way ANOVA with Sidak's multiple comparison test (**d**, **e**, **f**, **g**). Data are presented as the means +/- SEM. Statistical details are presented in Supplementary Data. 1 file. Source data are provided as a Source Data file.

Supplementary Fig. 25

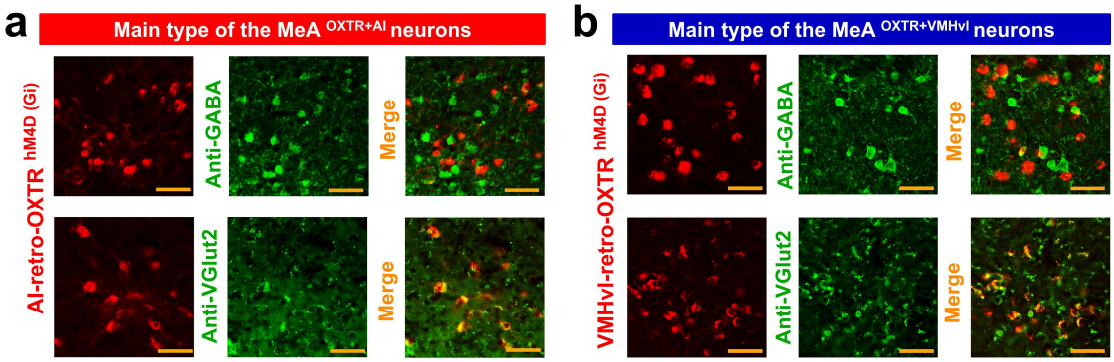

Supplementary Fig. 25 | The corresponding individual channels' images from representative overlapped images of hM4D (Gi) (mCherry, red) and VGlut2 (AF488, green) positive neurons, and Gi and GABA (AF488, green) positive neurons in the MeA$^{OXTR+AI}$ and MeA$^{OXTR+VMHvl}$.

a Overlapped images of GABA or VGlut2 positive cells and the MeA$^{OXTR+AI}$ cells. **b** Overlapped images of GABA or VGlut2 positive cells and the MeA$^{OXTR+VMHvl}$ cells. scale bars in all images, 50 μm.

Supplementary Fig. 26

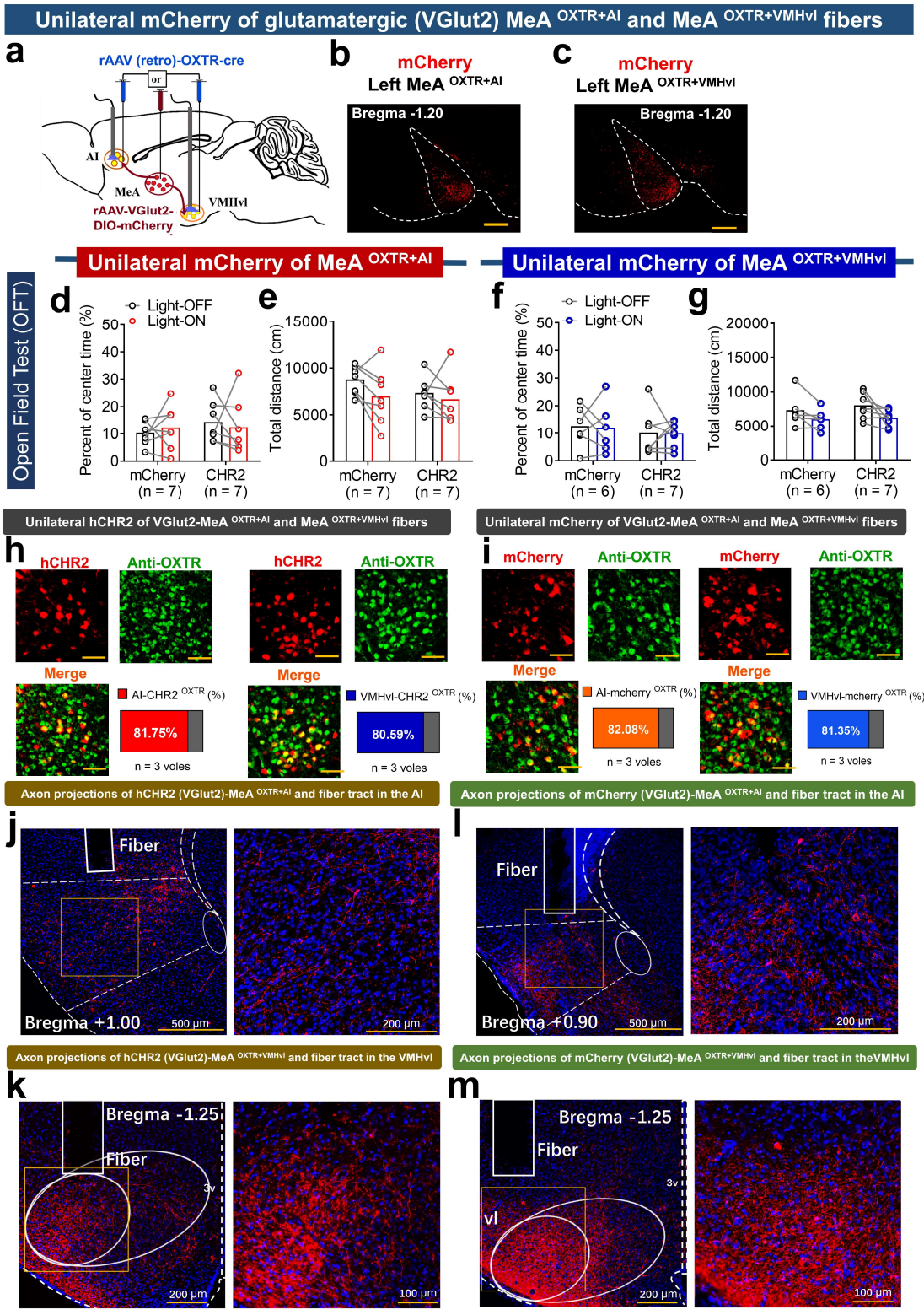

Supplementary Fig. 26 | Effects of optogenetic activation of fibers of the glutamatergic (VGlut2) MeA$^{OXTR+AI}$ and MeA$^{OXTR+VMHvl}$ on anxiety level and locomotion.

a Viral regimen for control experiment of CHR2 in fibers of the VGlut2-MeA$^{OXTR+AI}$ and MeA$^{OXTR+VMHvl}$ cells. Diagram was adapted from *The Mouse Brain in Stereotaxic Coordinates* by

Paxinos and Franklin. **b**, **c** Images of OXTR-mCherry expression (red) in the $MeA^{OXTR+AI}$ and $MeA^{OXTR+VMHvl}$. Scale bars, 500 μm. 7 and 6 independent repetitions with similar results in (**b**) and (**c**). **d**–**g** Behavioral distinction of percentage of center duration and total distance between the VGlut2-CHR2 and VGlut2-mCherry groups in $MeA^{OXTR+AI}$ fibers (**d**, **e**) and $MeA^{OXTR+VMHvl}$ fibers (**f**, **g**). n (mCherry) = 7 voles, n (CHR2) = 7 voles were used in VGlut2-CHR2 of the $MeA^{OXTR+AI}$ fibers (d and e); n (mCherry) = 6 voles, n(CHR2) = 7 voles were used in VGlut2-CHR2 of the $MeA^{OXTR+VMHvl}$ fibers (**f**, **g**). **h**, **i** The corresponding individual channels' images from representative overlapped images of hCHR2 (VGlut2)-$MeA^{OXTR+AI}$ somata and anti-OXTR cells and overlapped images of hCHR2 (VGlut2)-$MeA^{OXTR+VMHvl}$ somata and anti-OXTR cells, and overlapped images of mCherry (VGlut2)-$MeA^{OXTR+AI}$ somata and anti-OXTR cells and overlapped images of mCherry (VGlut2)-$MeA^{OXTR+VMHvl}$ somata and anti-OXTR cells. Scale bars, 50 μm. **j**, **k** Representative axon projections and fiber tract of VGlut2-hCHR2-$MeA^{OXTR+AI}$ and VGlut2-hCHR2-$MeA^{OXTR+VMHvl}$ in the AI and VMHvl. **l**, **m** Representative axon projections and fiber tract of VGlut2-mCherry-$MeA^{OXTR+AI}$ and VGlut2-mCherry-$MeA^{OXTR+VMHvl}$ in the AI and VMHvl. Data analyzed by Repeated measure two-way ANOVA with Sidak's multiple comparison test (**d**, **e**, **f**, **g**). Data are presented as the means +/- SEM. Statistical details are presented in Supplementary Data. 1 file. Source data are provided as a Source Data file. VGlut2 = vesicular glutamate transporter 2.

Supplementary Fig. 27

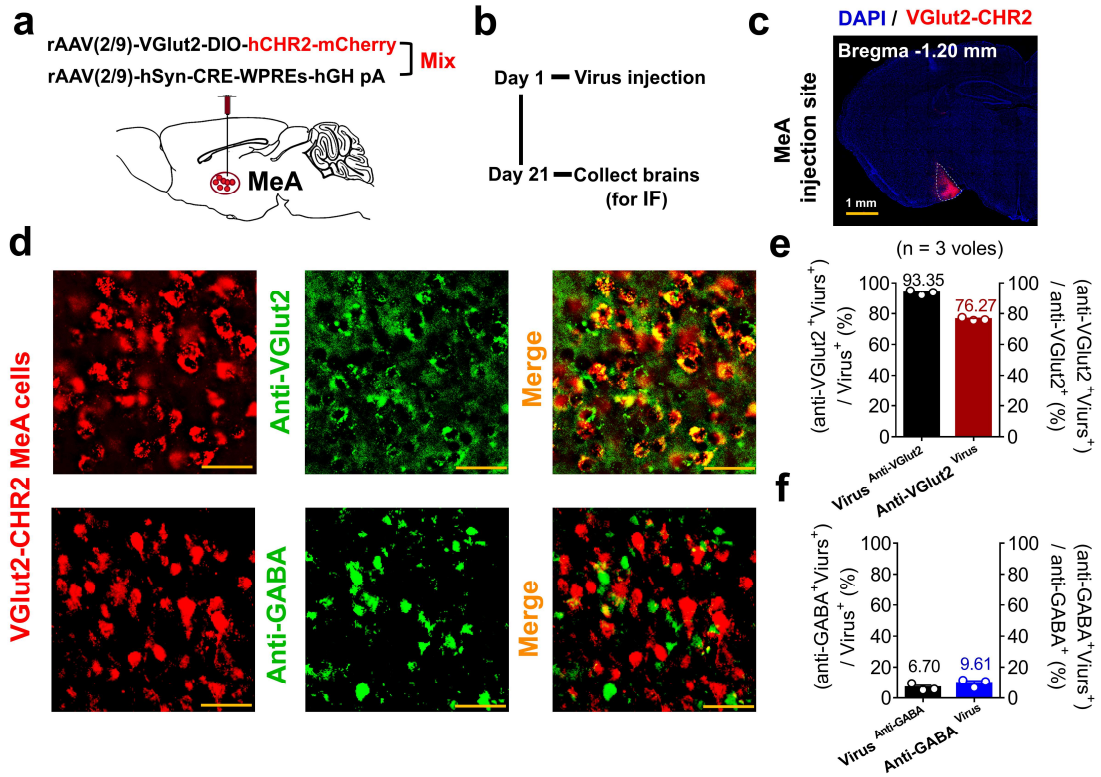

Supplementary Fig. 27 | The validation of the efficiency and specificity of rAAV-VGlut2-DIO-hCHR2-mCherry infection in the MeA.

a, **b** Virus regimen (adapted from *The Mouse Brain in Stereotaxic Coordinates* by Paxinos and Franklin. **a**) and schedule (**b**) were used to infect the glutamatergic (VGlut2$^+$) MeA neurons by co-injecting rAAV-VGlut2-DIO-hCHR2 with rAAV-hSyn-Cre into the MeA. **c** Representative image of VGlut2-mCherry (red) expression in the left MeA. scale bar, 1 mm. 3 independent repetitions with similar results in (**c**). **d** Representative images of VGlut2-CHR2$^+$ infected neurons (red) and Anti-VGlut2$^+$ / Anti-GABA$^+$ labeled cells (AF488, green) in the MeA. Scale bars, 50 μm. **e**, **f** Quantification of the percentage of VGlut2 (GABA) antibody-labeled VGlut2-CHR2$^+$ neurons in the total VGlut2-CHR2$^+$ infected cells (**e**), and quantification of the percentage of VGlut2-CHR2$^+$ infected cells in the total VGlut2 / GABA antibody-labeled cells (**f**). Data are presented as the means +/- SEM. Source data are provided as a Source Data file. VGlut2 = vesicular glutamate transporter 2. Mix = 200 nl of mixture of rAAV-VGlut2-DIO-hCHR2 and rAAV-CRE. IF = Immunofluorescence experiment.

Supplementary Fig. 28

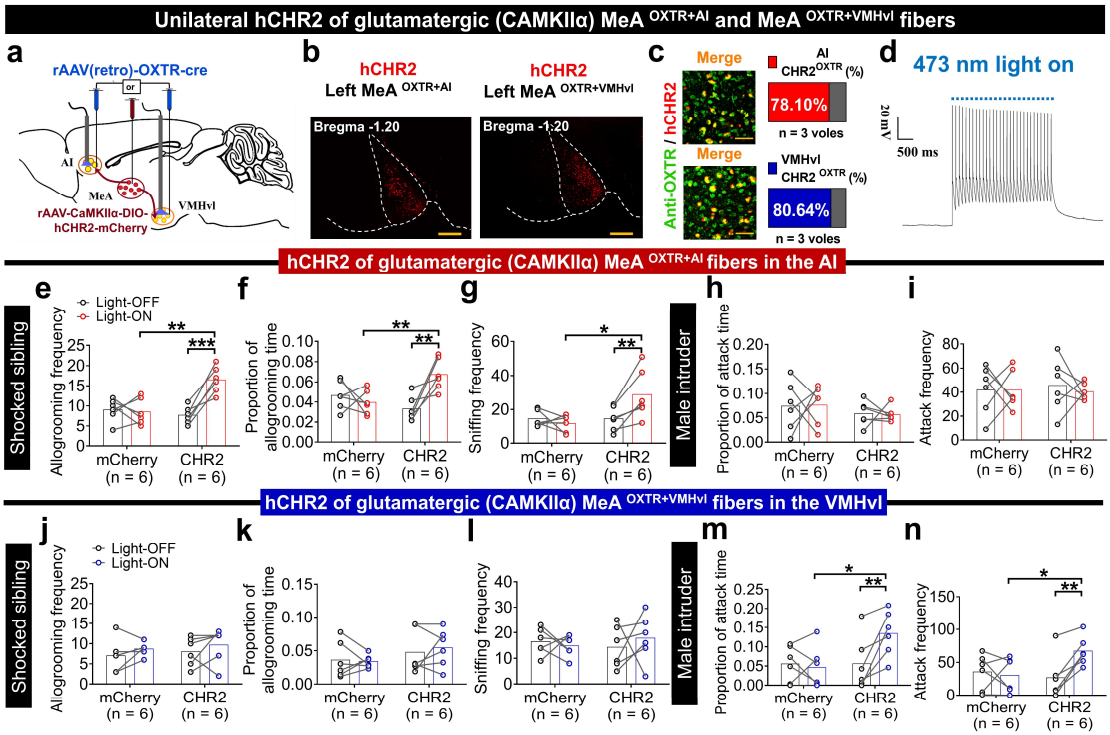

Supplementary Fig. 28 | The behavioral effect of optogenetic activation of fibers located in the AI or VMHvl of the glutamatergic (CAMKIIα)-MeA^{OXTR} neurons.

a Viral regimen for optogenetic activation of the glutamatergic (CAMKIIα) fibers. Diagram was adapted from *The Mouse Brain in Stereotaxic Coordinates* by Paxinos and Franklin. **b** Images of hCHR2 expression (red). Scale bars, 500 μm. **c** Representative overlapped images of CAMKIIα-hCHR2 (red) and anti-OXTR (AF488, green) cells. Scale bars, 50 μm; n = 3 voles / group. **d** Representative electrophysiological traces showing photoactivation effect. **e**–**i**, **j**–**n** Comparison of allogrooming (**e**, **f**, **j**, **k**) and sniffing siblings (**g**, **l**), and attacking intruders (**h**, **i**, **m**, **n**) between the CAMKIIα-hCHR2 and CAMKIIα-mCherry groups in the MeA$^{OXTR+AI}$ and MeA$^{OXTR+VMHvl}$. n = 6 voles / group in (**e**–**n**). In (**e**–**i**), allogrooming frequency: CHR2-Light OFF versus CHR2-Light ON, p = 0.0002; mcherry-Light ON versus CHR2-Light ON, p = 0.002; allogrooming time proportion: CHR2-Light OFF versus CHR2-Light ON, p = 0.004; mcherry-Light ON versus CHR2-Light ON, p = 0.007; sniffing frequency: CHR2-Light OFF versus CHR2-Light ON, p = 0.003; mcherry-Light ON versus CHR2-Light ON, p = 0.022. In (**j**–**n**), attack time proportion: CHR2-Light OFF versus CHR2-Light ON, p = 0.005; mcherry-Light ON versus CHR2-Light ON, p = 0.023; attack frequency: CHR2-Light OFF versus CHR2-Light ON, p = 0.004; mcherry-Light ON versus CHR2-Light ON, p = 0.026. Data analyzed by Repeated measure two-way ANOVA with Sidak's multiple comparison test (**e**–**n**). $^{***}p < 0.001$, $^{**}p < 0.01$, $^{*}p < 0.05$. Data are presented as the means +/- SEM. Statistical details are presented in Supplementary Data. 1 file. Source data are provided as a Source Data file. CAMKIIα = Calcium–calmodulin (CaM)-dependent protein kinase IIα.

Supplementary Fig. 29

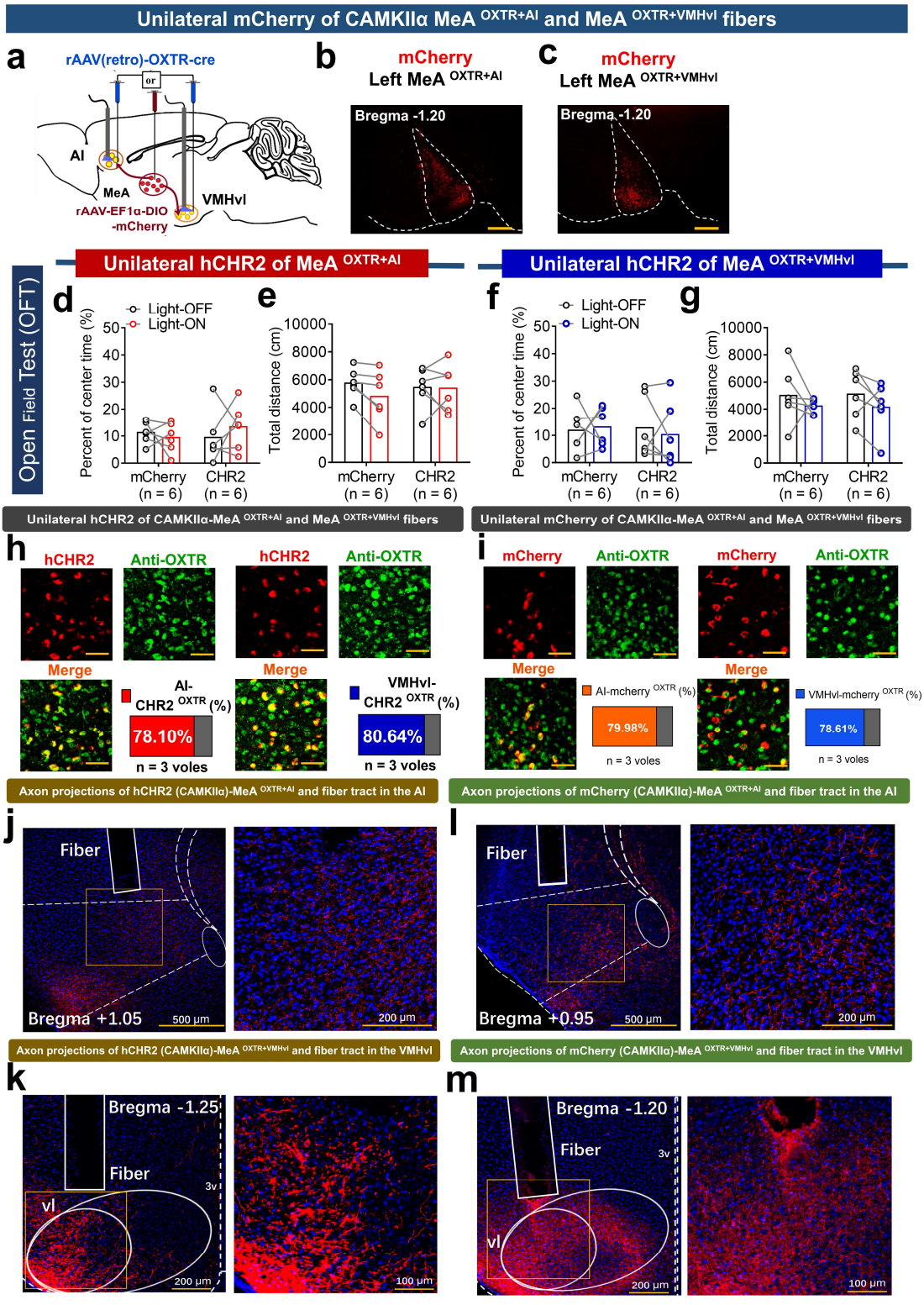

Supplementary Fig. 29 | Effects of optogenetic activation of fibers of the glutamatergic (CAMKIIα) MeA$^{OXTR+AI}$ and MeA$^{OXTR+VMHvl}$ on anxiety level and locomotion.

a Viral regimen for control experiment of CHR2 in fibers of the CAMKIIα-MeA$^{OXTR+AI}$ and MeA$^{OXTR+VMHvl}$ cells. Diagram was adapted from *The Mouse Brain in Stereotaxic Coordinates* by Paxinos and Franklin. **b**, **c** Images of OXTR-mCherry (red) expression in the MeA$^{OXTR+AI}$ and

$MeA^{OXTR+VMHvl}$. Scale bars, 500 μm. 6 independent repetitions with similar results in (**b**) and (**c**). **d**–**g** Behavioral distinction of percentage of center duration and total distance between the CAMKIIα-CHR2 and CAMKIIα-mCherry groups in $MeA^{OXTR+AI}$ fibers (**d**, **e**) and $MeA^{OXTR+VMHvl}$ fibers (f and g). n (mCherry) = 6 voles, n (CHR2) = 7 voles were used in CAMKIIα-CHR2 of the $MeA^{OXTR+AI}$ fibers (**d**, **e**); n (mCherry) = 6 voles, n (CHR2) = 6 voles were used in CAMKIIα-CHR2 of the $MeA^{OXTR+VMHvl}$ fibers (**f**, **g**). **h**, **i** The corresponding individual channels' images from representative overlapped images of hCHR2 (CAMKIIα)-$MeA^{OXTR+AI}$ somata and anti-OXTR cells and overlapped images of hCHR2 (CAMKIIα)-$MeA^{OXTR+VMHvl}$ somata and anti-OXTR cells, and overlapped images of mCherry (CAMKIIα)-$MeA^{OXTR+AI}$ somata and anti-OXTR cells and overlapped images of mCherry (CAMKIIα)-$MeA^{OXTR+VMHvl}$ somata and anti-OXTR cells. **j**, **k** Representative axon projections and fiber tract of CAMKIIα-hCHR2-$MeA^{OXTR+AI}$ and CAMKIIα-hCHR2-$MeA^{OXTR+VMHvl}$ in the AI and VMHvl. **l**, **m** Representative axon projections and fiber tract of CAMKIIα-mCherry-$MeA^{OXTR+AI}$ and CAMKIIα-mCherry-$MeA^{OXTR+VMHvl}$ in the AI and VMHvl. Data analyzed by Repeated measure two-way ANOVA with Sidak's multiple comparison test (**d**, **e**, **f**, **g**). Data are presented as the means +/- SEM. Statistical details are presented in Supplementary Data. 1 file. Source data are provided as a Source Data file. CAMKIIα = Calcium–calmodulin (CaM)-dependent protein kinase IIα.

Supplementary Fig. 30

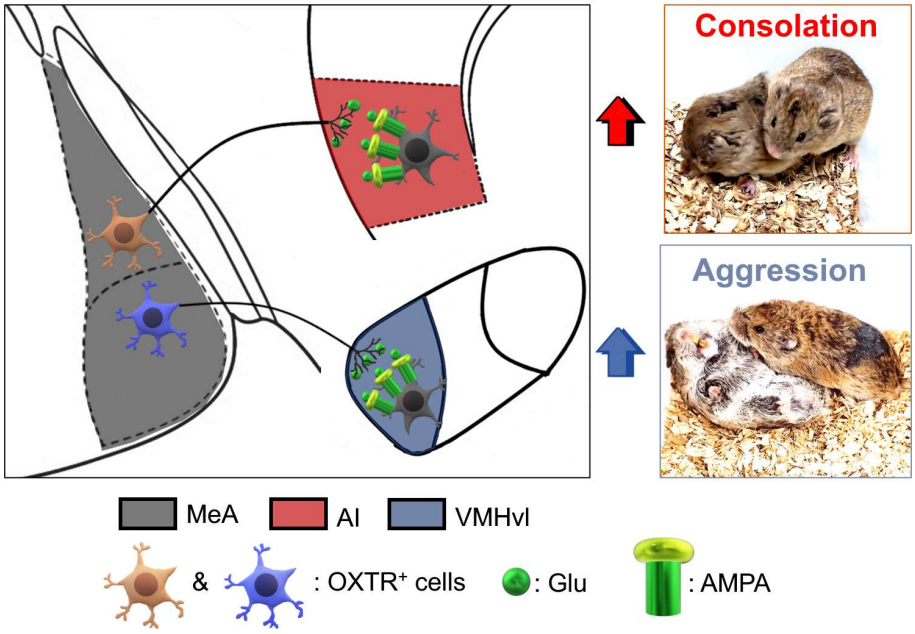

Supplementary Fig. 30 | Graphic summary of finding in the present study: OXTR neurons in the MeA projecting to the AI or VMHvl regulate consolation and aggression through glutaminergic mechanism respectively.

Diagram was adapted from *The Mouse Brain in Stereotaxic Coordinates* by Paxinos and Franklin. MeA = medial amygdala; AI = anterior insula; VMHvl = ventrolateral aspect of ventromedial hypothalamus; OXTR = oxytocin receptor; Glu = Glutamic acid; AMPA = α-amino-3-hydroxy-5-methyl-4-isoxazole-propionic acid receptors.

Supplementary Fig. 31

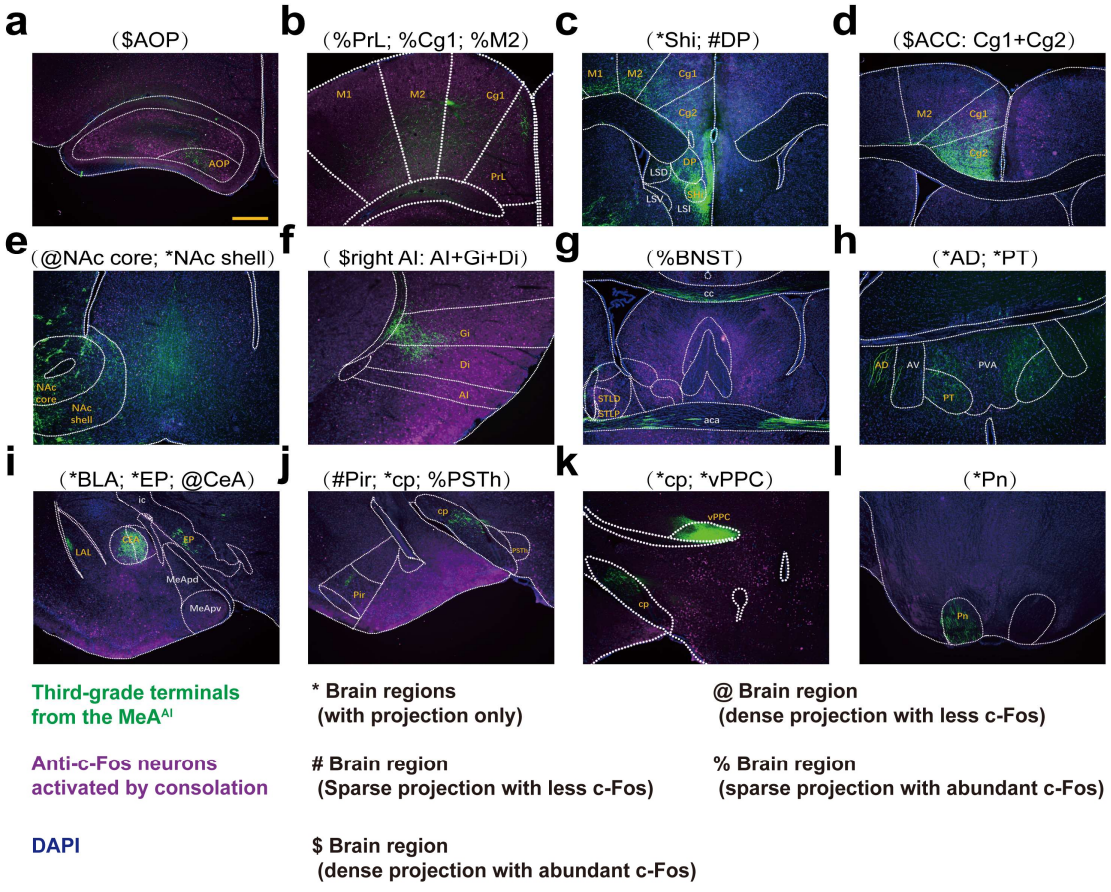

Supplementary Fig. 31 | Representative overlapped images of the third-grade projected regions from the MeA^{AI}, and positive c-Fos neurons activated by consolation.

Third-grade terminals, c-Fos positive neurons and DAPI were showed as green, magenta and blue, respectively. 3 independent repetitions with similar results. AOP = anterior olfactory area posterior part; PrL = prelimbic cortex; Cg1 = cingulate cortex, area 1; M2 = secondary motor cortex; Shi = septohippocampal nucleus; DP = dorsal peduncular cortex; Cg2 = cingulate cortex, area 2; NAc core = accumbens nucleus, core; NAc shell = accumbens nucleus, shell; Gi = gigantocellular reticular nucleus; Di = dysgranular insular cortex; AI = agranular insular cortex; BNST = bed nucleus of the stria terminalis; AD = anterodorsal thalamic nucleus; PT = paratenial thalamic nucleus; BLA = basolateral amygdaloid nucleus, anterior part; EP = entopeduncular nucleus; CeA = central amygdala; Pir = piriform cortex; cp = cerebral peduncle; PSTh = parasubthalamic nucleus; vPPC = ventral posterior nucleus of the thalamus, parvicellular part; Pn = pontine nuclei. Scale bars in (**a**) for all images, 500 μm.

Supplementary Fig. 32

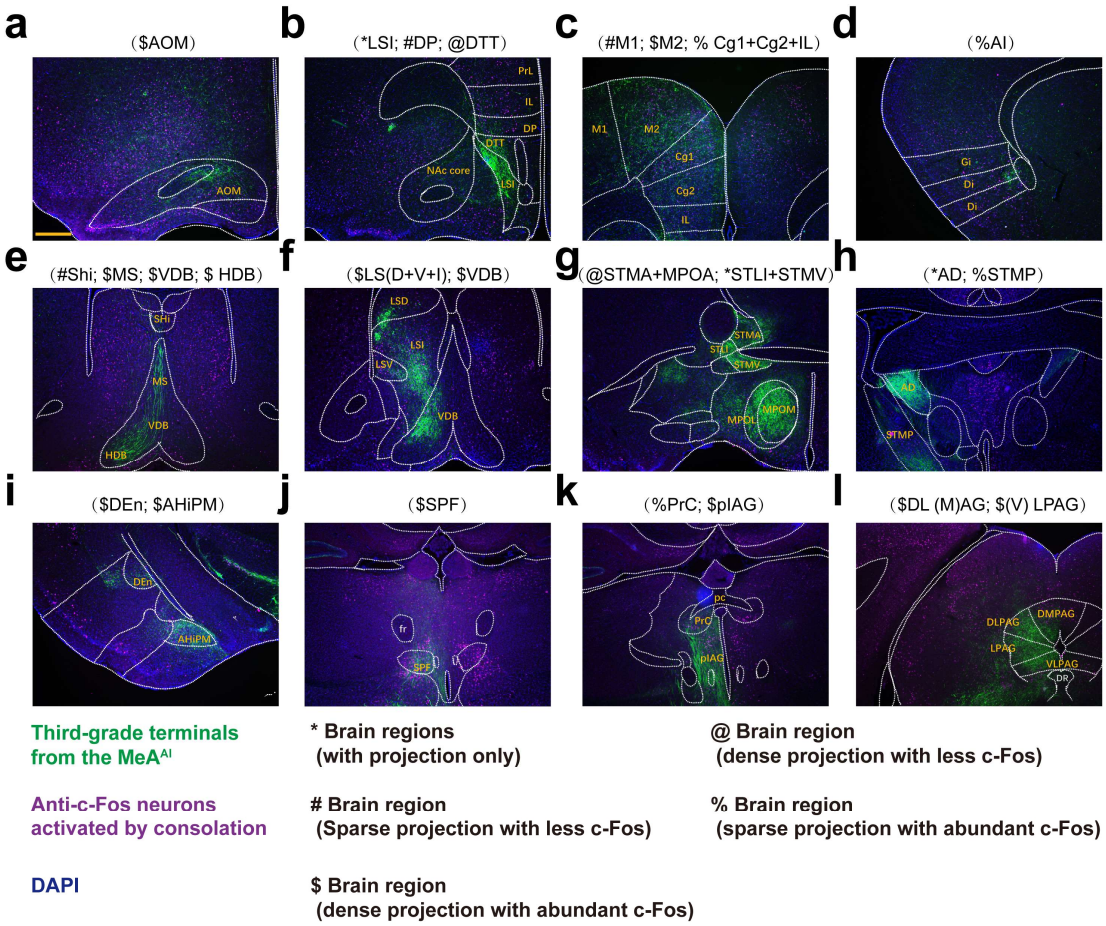

Supplementary Fig. 32 | Representative overlapping images of the third-grade projected regions from the MeA^{VMHvl}, and positive c-Fos neurons activated by aggression.
Third-grade terminals, c-Fos positive neurons and DAPI were showed as green, magenta and blue, respectively. 3 independent repetitions with similar results. AOM = anterior olfactory area, medial part; LS = lateral septal nucleus; DTT = dorsal tenia tecta; IL = infralimbic cortex; MS = medial septal nucleus; VDB = nucleus of the vertical limb of the diagonal band; HDB = nucleus of the horizontal limb of the diagonal band; MPOA = Medial preoptic area; Den = dorsal endopiriform claustrum; AHiPM = amygdalohippocampal area, posteromedial part; SPF = subparafascicular thalamic nucleus; PrC = precommissural nucleus; PAG = periaqueductal gray. Scale bars in (**a**) for all images, 500 μm.

Supplementary Tables

Supplementary Table. 1

Behavioral test	indicators	Definition for recording / measuring
Consolation test	Sniff sibling	Using nose to inspect any portion of the sibling's body, including the nose, head, tail and anogenital areas.
	Allogroom sibling	Head contact with the body or head of subjects' sibling, accompanied by a rhythmic head movement.
Resident-intruder paradigm	Sniffing intruder	Using nose to inspect any portion of the intruder's body, including the nose, head, tail and anogenital areas.
	Attack intruder	A series of actions initiated by the subjects to the intruders, including body swaying back and forth for claiming lordship, bites, pinning, tumbling and quick chasing for attack or eviction between these behaviors.
New object recognition model	Sniff object	Using nose to inspect the surface of object (rubik's Cube).

Supplementary Table. 1 | Definition of main behavioral indicators in consolation test, resident-intruder paradigm and new object recognition model.

Supplementary Notes

Supplementary Note 1

Our previous studies had revealed that mandarin voles displayed allogrooming towards distressed partners as a stress buffering behavior [1, 2]. However, it is unknown whether allogrooming and its buffering effect exists between male sibling voles. To answer this question, male voles (siblings) subjected to electric foot shock were then randomly exposed to sibling subjects (the Reunion group) or alone (the Shock group) for 10 min, the group-housed voles (the Con group) without any treatment were included (Supplementary Fig. 2a–c). Finally, behavioral performance in 25-min open field test (OFT) [3] and serum CORT levels [4] of siblings after treatments were all detected to evaluate stressed level. As we expected, the Shock group showed significantly increased time in the corners than the Con and Reunion groups during 25-min OFT (Supplementary Fig. 2d). The Shock group also showed higher serum CORT level than the other two groups (Supplementary Fig. 2e). In addition, there was a significant positive correlation between the corner time and serum CORT level (Supplementary Fig. 2f). These results confirmed the stress buffering effect of allogrooming between male sibling voles, which laid a foundation for subsequent application of the consolation test.

Supplementary Note 2

We injected rAAV2/9-CAG-mWGA-mCherry in the MeA to anterogradely trace downstream monosynaptic neurons (Supplementary Fig. 7a and b), then quantified co-labeled AI^{MEA} / $VMHvl^{MEA}$ (mCherry, red) and c-Fos positive neurons under different treatments to further confirm the results by the above-mentioned AAV (2/1) strategy. As shown in Supplementary Fig. 7e–h and i–l, the Consolation and Aggression groups had specifically higher percentage of co-labeling neurons in the AI and VMHvl, respectively (Supplementary Fig. 7c and d). The activities ratio of AI^{MEA} / $VMHvl^{MEA}$ in the Separation, Control, consolation and aggression groups did not show significant difference between two strategies using AAV (2/1) and CAG-mWGA as anterograde tracer (Supplementary Fig. 7m and n). Further, rAAV2/9-CAG-EGFP was injected to the AI or VMHvl (Supplementary Fig. 8a–f), however there are rare axon projections to the MeA from the AI and VMHvl somata respectively (Supplementary Fig. 8g–j).

Supplementary Note 3

30 days after injection of rAAV2/9-OXTR-mCherry into the MeA (Supplementary Fig. 11d–f), we compared OXTR neurons fibers density between the AI (Supplementary Fig. 11h), the reported medial preoptic area (MPOA, Supplementary Fig. 11i) associated with consolation [3], VMHvl (Supplementary Fig. 11j) and the classic bed nucleus of the stria terminalis (BNST, Supplementary Fig. 11k) associated with aggression [5]. No difference in fiber's integrated optical density (IOD) of OXTR neurons was found between the AI and MPOA, or between the VMHvl and BNST (Supplementary Fig. 11g). This result indicated that densities of the MeA OXTR neurons projections to AI, MPOA, BNST and VMHvl were similar.

Supplementary Discussion

Noticeably, Hong et al. [6] showed that the activation of the whole GABAergic PD subregion of the MeA neurons could also promote aggression. In our study, the MeA neurons were considered to be both "VMHvl-projecting" and "OXTR expressing". These $MeA^{OXTR+VMHvl}$ neurons that specifically regulate aggression only account for 36.43% of the whole MeA glutamatergic neurons (Fig. 9f). 24.34% of the $MeA^{OXTR+VMHvl}$ neurons are GABAergic (Fig. 9h). Accordingly, we assumed both GABAergic and glutamatergic neurons could regulate aggression through interaction or co-regulation mechanism, which needed to be clarified in the future. In addition, the influences of sexual experience on sex-specific aggression are both reflected in the VMHvl [7] and OXT signaling of the MeA [8], whether and how $MeA^{OXTR+VMHvl}$ neurons mediate such influences became a next open question. Finally, we discovered that resident male voles with ablation of the $MeA^{OXTR+VMHvl}$ exhibited few or even no attack to none-aggressive intruder voles. One possible explanation is that ablation of the $MeA^{OXTR+VMHvl}$ may cause less emission of aggression-promoting pheromones including 2-(sec-butyl)-dihydrothiazole and dehydro-exo-brevicomin and major urinary proteins (MUP) to further weaken residents' aggression [9]. According to social status-related behavioral effect of OXT in aggression [10], inhibition of the $MeA^{OXTR+VMHvl}$ may decrease social dominance that result in reduction of aggression. These hypotheses need to be proved in the future study.

Finally, the supplementary results of anterograde monosynaptic tracing needed to be pointed out. By this scheme, EGFP-marked AI or VMHvl somata receiving monosynaptic projections from the MeA could send out monosynaptic fibers marked by EGFP to downstream regions (third-grade regions). We co-labeled EGFP-marked third-grade regions with c-Fos under consolation or aggression to expand the possible circuits of the MeA-AI and MeA-VMHvl involved in the consolation or aggression respectively. The posterior part of anterior olfactory area (AOP), prelimbic cortex (Prl), anterior cingulate cortex (ACC), nucleus accumbens (NAc) core and shell, BNST, central amygdala (CeA) and contralateral AI regions that received MeA-AI projections expressed high levels of c-Fos under consolation (Supplementary Fig. 31). The activated anterior olfactory area (AOM), secondary motor cortex (M2), ACC, lateral septal nucleus (LS) and nucleus of the vertical limb of the diagonal band (VDB), BNST, subparafascicular thalamic nucleus (SPF) and periaqueductal gray (PAG) that receiving MeA-VMHvl projections were also found (Supplementary Fig. 32). However, whether and how these "MeA-AI/VMHvl-third-grade region" neuronal circuits regulate corresponding behaviors and the roles of the OXT system in these circuits are also needed to be clarified further.

Supplementary References

1. Li L*, et al.* Dorsal raphe nucleus to anterior cingulate cortex 5-HTergic neural circuit modulates consolation and sociability. *eLife* **10**, (2021).
2. Li LF*, et al.* Reduced Consolation Behaviors in Physically Stressed Mandarin Voles: Involvement of Oxytocin, Dopamine D2, and Serotonin 1A Receptors Within the Anterior Cingulate Cortex. *Int J Neuropsychopharmacol* **23**, 511-523 (2020).
3. Wu YE*, et al.* Neural control of affiliative touch in prosocial interaction. *Nature* **599**, 262-267 (2021).
4. Li LF*, et al.* Involvement of oxytocin and GABA in consolation behavior elicited by socially defeated individuals in mandarin voles. *Psychoneuroendocrinology* **103**, 14-24 (2019).
5. Nordman JC*, et al.* Potentiation of Divergent Medial Amygdala Pathways Drives Experience-Dependent Aggression Escalation. *The Journal of neuroscience : the official journal of the Society for Neuroscience* **40**, 4858-4880 (2020).
6. Hong W, Kim DW, Anderson DJ. Antagonistic control of social versus repetitive self-grooming behaviors by separable amygdala neuronal subsets. *Cell* **158**, 1348-1361 (2014).
7. Lin D*, et al.* Functional identification of an aggression locus in the mouse hypothalamus. *Nature* **470**, 221-226 (2011).
8. Li Y*, et al.* Neuronal Representation of Social Information in the Medial Amygdala of Awake Behaving Mice. *Cell* **171**, 1176-1190.e1117 (2017).
9. Liberles SD. Mammalian pheromones. *Annual review of physiology* **76**, 151-175 (2014).
10. Winslow JT, Insel TR. Social status in pairs of male squirrel monkeys determines the behavioral response to central oxytocin administration. *The Journal of neuroscience : the official journal of the Society for Neuroscience* **11**, 2032-2038 (1991).